

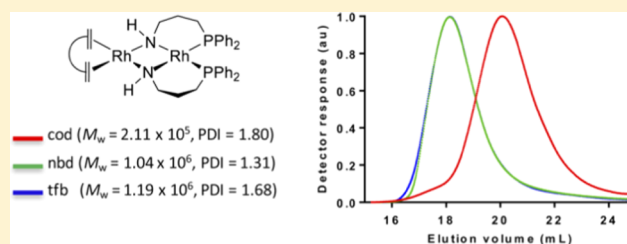
Dinuclear Phosphine-Amido $[\text{Rh}_2(\text{diene})\{\mu\text{-NH}(\text{CH}_2)_3\text{PPh}_2\}_2]$ Complexes as Efficient Catalyst Precursors for Phenylacetylene Polymerization

Marta Angoy, M. Victoria Jiménez,*^{1b} Pilar García-Orduña, Luis A. Oro,^{1b} Eugenio Vispe, and Jesús J. Pérez-Torrente*^{1b}

Departamento de Química Inorgánica, Instituto de Síntesis Química y Catálisis Homogénea–ISQCH, Universidad de Zaragoza–CSIC, Facultad de Ciencias, C/Pedro Cerbuna, 12, 50009 Zaragoza, Spain

S Supporting Information

ABSTRACT: Dinuclear phosphine-amido, $[\text{Rh}_2(\text{diene})\{\mu\text{-NH}(\text{CH}_2)_3\text{PPh}_2\}_2]$, and cationic phosphine-amino complexes, $[\text{Rh}(\text{diene})\{\text{Ph}_2\text{P}(\text{CH}_2)_3\text{NHR}\}]^+$ (diene = cod, nbd, tfb) and $[\text{Rh}\{\text{Ph}_2\text{P}(\text{CH}_2)_3\text{NHR}\}_2]^+$, have been prepared from the corresponding amino-functionalized phosphines $\text{Ph}_2\text{P}(\text{CH}_2)_3\text{NHR}$ (R = H, Me) and suitable rhodium(I) precursors. The dinuclear $[\text{Rh}_2(\text{diene})\{\mu\text{-NH}(\text{CH}_2)_3\text{PPh}_2\}_2]$ complexes bearing π -acceptors diene ligands such as nbd or tfb exhibit a remarkable catalytic activity in phenylacetylene (PA) polymerization affording stereoregular polyphenylacetylenes with, unlike the cod precursor, unimodal molar mass distributions of very high molecular weights, M_w up to $\approx 1.2 \times 10^6$, and moderate polydispersity indexes. These complexes are more active than the mononuclear phosphino-anilido $[\text{Rh}(\text{diene})\{\text{Ph}_2\text{P}(\text{C}_6\text{H}_4)\text{NMe}_2\}]^+$ complexes, which are in turn more active than the cationic complexes $[\text{Rh}(\text{diene})\{\text{Ph}_2\text{P}(\text{CH}_2)_3\text{NHMe}\}]^+$, $[\text{Rh}(\text{nbd})\{\text{Ph}_2\text{P}(\text{CH}_2)_3\text{NH}_2\}]^+$, and $[\text{Rh}(\text{nbd})\{\text{Ph}_2\text{P}(\text{C}_6\text{H}_4)\text{NHMe}\}]^+$ bearing the same diene ligand. In contrast, complexes $[\text{Rh}\{\text{Ph}_2\text{P}(\text{CH}_2)_3\text{NHR}\}_2]^+$ (R = H, Me) without a diene ligand have been found to be inactive in PA polymerization. The excellent catalytic performance of $[\text{Rh}_2(\text{diene})\{\mu\text{-NH}(\text{CH}_2)_3\text{PPh}_2\}_2]$ (diene = nbd, tfb) complexes is a consequence of the mode of activation of PA that likely results in the formation of unsaturated alkynyl species $[\text{Rh}(\text{diene})(\text{C}\equiv\text{C-Ph})\text{L}]$ (L = PA, THF), which may be competent for PA polymerization.



INTRODUCTION

Polyphenylacetylene (PPA) and its derivatives are among the most widely studied polyene materials because of their stability in air, solubility in a range of organic solvents, and semiconductor properties. The rational selection of substituted acetylenes has directed the preparation of functional polymers with applications in electronics, photoelectronics, optics, and membrane separation.^{1,2} PPAs are produced mainly by chain growth polymerization of substituted phenylacetylene (PA) monomers with a suitable transition-metal catalyst. The oxophilic character of most early transition-metal-based catalysts results in a limited tolerance to functional groups in the monomers.³ In contrast, late transition-metal catalysts have drawn considerable attention because of their high activity, stability toward air and moisture, and the relatively wide range of applicable monomers due to the high tolerance to many of the heteroatoms in functional groups.^{4,5} In particular, rhodium catalysts efficiently catalyze the polymerization of monosubstituted acetylenes with the formation of highly stereoregular PPAs, in some cases in a living manner.^{6–8}

We have shown that cationic rhodium(I) complexes $[\text{Rh}(\text{diene})\{\text{Ph}_2\text{P}(\text{CH}_2)_n\text{Z}\}]^+$ containing functionalized phosphine ligands of hemilabile character of the type $\text{Ph}_2\text{P}(\text{CH}_2)_n\text{Z}$ ($n = 2$ or 3 ; $Z = \text{OMe}, \text{NMe}_2$) efficiently catalyze the

polymerization of PA affording very high-molecular-weight stereoregular PPA with a cis-transoidal configuration and moderate polydispersity indexes.⁹ In addition, characterization of the polymers by size exclusion chromatography, multiangle light scattering (SEC-MALS), or asymmetric flow field flow fractionation (A4F-MALS) has shown that some of these PPA samples contain a mixture of linear and branched polymers.¹⁰ Spectroscopic studies on the PA polymerization mechanism by the catalyst precursor $[\text{Rh}(\text{cod})\{\text{Ph}_2\text{P}(\text{CH}_2)_3\text{NMe}_2\}]^+$ led us to observe the alkynyl species $[\text{Rh}(\text{C}\equiv\text{C-Ph})(\text{cod})\{\text{Ph}_2\text{P}(\text{CH}_2)_3\text{NHMe}_2\}]^+$ formed by the intramolecular proton transfer from a η^2 -alkyne ligand to the uncoordinated $-\text{NMe}_2$ group, which acts as an internal base.⁹ This cationic alkynyl intermediate is the initiating species likely involved in the generation of stable rhodium-vinyl species responsible for the propagation step. In addition, mechanistic studies on PA polymerization by 2-diphenylphosphinopyridine-based rhodium(I) catalysts have allowed us to disclose the key role of rhodium-alkynyl species such as $[\text{Rh}(\text{C}\equiv\text{CPh})(\text{cod})\text{-}(\text{Ph}_2\text{PPy})]$ in the polymerization reaction.¹¹

Received: February 6, 2019

Based on these results, we anticipate that the introduction of anionic ligands derived from weak Brønsted acids in the coordination sphere of the metal center could be a fruitful strategy for the design of efficient polymerization catalysts as they could promote the formation of active alkynyl species by PA deprotonation. However, only a few rhodium(I) PA polymerization catalysts featuring functionalized anionic ligands have been reported to date. The neutral mononuclear complexes $[\text{Rh}(\text{acac})(\text{diene})]$,^{12,13} $[\text{Rh}(\text{AAEMA})(\text{diene})]$,¹³ and $[\text{Rh}(\text{L-alaninate})(\text{diene})]$ ¹⁴ (acac = acetylacetonate; AAEMA = deprotonated form of 2-(acetoacetoxy)-ethylmethacrylate) efficiently polymerize PA in the absence of any co-catalyst. In contrast, the catalytic system based on $[\text{Rh}(\text{quinol})(\text{diene})]$ (quinol = 8-quinolinolate), generated in situ by reaction of $[\text{Rh}(\mu\text{-OMe})(\text{diene})]_2$ with 8-hydroxyquinoline, requires an external base as co-catalyst (piperidine) to activate the system.¹⁵ In this context, rhodium(I) amido complexes have great potential as polymerization initiators due to the presence of very basic amido ligands that can behave as strong internal base for the deprotonation of PA.

Late transition-metal amido complexes have attracted a great deal of attention in part because of their potential participation in catalytic processes and important organic transformations.^{16–18} In contrast to early transition-metal amido complexes in which the π -bonding is significant, repulsive filled $p\pi$ – $d\pi$ electronic repulsions in late transition-metal amido complexes prevent charge delocalization, which confers the N atom a high basicity and nucleophilicity. The design of PNP pincer ligands has allowed the development of the late-metal amido organometallic chemistry. The pioneering work by Fryzuk et al. demonstrated the ability of rhodium and iridium complexes with a PNP pincer ligand with a disililamido scaffold to heterolitically activate molecular H_2 by transferring a proton to the amido group.¹⁹ In fact, this contribution was later recognized as the key in the design of bifunctional catalysts exhibiting metal–ligand cooperativity.²⁰

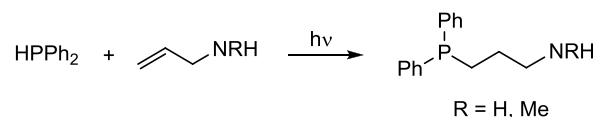
To the best of our knowledge, the only rhodium(I) amido compound reported as catalyst for PA polymerization is the phosphinosulfonamido $[\text{Rh}(\text{cod})(\text{Ph}_2\text{PCH}_2\text{CH}_2\text{NTs})]$ (Ts = $\text{SO}_2\text{C}_6\text{H}_4$ -*p*-Me) complex. This catalyst polymerizes PA in organic solvents such as CH_2Cl_2 , benzene, and THF to afford polymers of M_w in the range of $(6.32\text{--}2.86) \times 10^4$ without the need for co-catalyst.²¹ We report herein on the synthesis, characterization, and application in PA polymerization of a range of neutral mono- and dinuclear phosphino-amido complexes, $[\text{Rh}(\text{diene})\{\text{Ph}_2\text{P}(\text{C}_6\text{H}_4)\text{NMe}\}]$ and $[\text{Rh}_2(\text{diene})\{\mu\text{-NH}(\text{CH}_2)_3\text{PPh}_2\}_2]$, respectively. In addition, the catalytic activity of a series of cationic complexes, $[\text{Rh}(\text{diene})\{\text{Ph}_2\text{P}(\text{CH}_2)_3\text{NHR}\}]^+$ (R = H, Me), based on new phosphino-amino ligands has been also studied for comparative purposes.

RESULTS AND DISCUSSION

Synthesis of Amino-Functionalized Phosphines. The functionalized phosphines $\text{Ph}_2\text{P}(\text{CH}_2)_3\text{Z}$ (Z = NHMe, NH_2) have been prepared by the photochemical hydrophosphination method using suitable functionalized allyl derivatives.²² Reaction of HPPH_2 with an excess of the corresponding allylamine $\text{H}_2\text{C}=\text{CHCH}_2\text{Z}$ (Z = NHMe, NH_2) under visible light for 5 days at room temperature without any solvent directly afforded the amino-functionalized phosphines, which were isolated as colorless oils after removing the remaining allylamine under vacuum. The reactions proceed in an efficient and regioselective way to exclusively give the anti-Markonikov

addition products (Scheme 1). The new phosphines 3-(diphenylphosphino)-*N*-methylpropan-1-amine (Ph_2P -

Scheme 1. Synthesis of Amino-Functionalized Phosphines

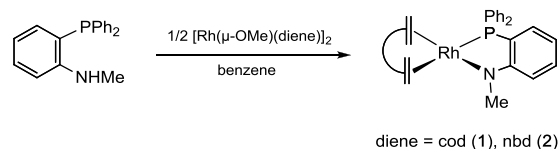


(CH_2)₃NHMe) and 3-(diphenylphosphino)propan-1-amine ($\text{Ph}_2\text{P}(\text{CH}_2)_3\text{NH}_2$) were isolated in 82 and 77% yields, respectively, and have been characterized by elemental analysis, mass spectrometry (ESI-MS), and NMR spectroscopy.

The $^{31}\text{P}\{^1\text{H}\}$ NMR spectrum of both compounds in CDCl_3 showed a singlet resonance at δ –15.6 and –16.0 ppm, respectively. A set of three resonances for the $>\text{CH}_2$ of the alkylamino chain was observed between δ 2.8 and 1.6 ppm in the ^1H NMR spectra, with the most deshielded resonance that of the methylene group attached to the nitrogen heteroatom. The resonances of the amine protons of the $-\text{NH}_2$ and $-\text{NHMe}$ groups were observed as broad resonances around $\delta \approx 1.25$ ppm. Finally, the *N*-methyl group of the aminophosphine $\text{Ph}_2\text{P}(\text{CH}_2)_3\text{NHMe}$ was observed at δ 2.41 and 36.40 ppm in the ^1H and $^{13}\text{C}\{^1\text{H}\}$ NMR spectra, respectively.

Synthesis of Mono- and Dinuclear Phosphine-Amido Rhodium(I) Complexes. The acidic proton of 2-(diphenylphosphino)-*N*-methylaniline can be easily deprotonated by the basic methoxo bridged ligands of the dinuclear compounds $[\text{Rh}(\mu\text{-OMe})(\text{diene})]_2$ to give square-planar mononuclear phosphine-anilido $[\text{Rh}(\text{diene})\{\text{Ph}_2\text{P}(\text{C}_6\text{H}_4)\text{NMe}\}]$ complexes (Scheme 2). We have applied this methodology, established by

Scheme 2. Synthesis of Phosphine-Anilido Mononuclear Complexes



diene = cod (1), nbd (2)

Cowie et al., for the synthesis of $[\text{Rh}(\text{cod})\{\text{Ph}_2\text{P}(\text{C}_6\text{H}_4)\text{NMe}\}]$ (1),²³ to the preparation of the related compound $[\text{Rh}(\text{nbd})\{\text{Ph}_2\text{P}(\text{C}_6\text{H}_4)\text{NMe}\}]$ (2), which was obtained as an orange solid in 73% yield.

The MALDI-TOF mass spectrum of **2** featured a peak at an m/z ratio of 486.0 for the protonated molecular ion. The $^{31}\text{P}\{^1\text{H}\}$ NMR spectrum in C_6D_6 showed a doublet at δ 38.4 ppm with a $J_{\text{P-Rh}}$ of 183 Hz, significantly larger than that found in **1** (163 Hz), in agreement with the higher π -acceptor character of the nbd diene ligand. The ^1H NMR spectrum does not show the characteristic NH signal of the aminophosphine ligand, which supports the formation of an amido complex. The number of resonances observed in the spectrum is in accordance with the formation of a mononuclear compound of C_s symmetry derived from the bidentate $\kappa^2\text{P}_2\text{N}$ coordination of amido-phosphine ligand. In particular, the olefinic protons of the 2,5-norbornadiene ligand were observed as two broad resonances at δ 4.85 and 3.25 ppm due to the different coordination atom in trans position. This fact is also reflected in the $^{13}\text{C}\{^1\text{H}\}$ NMR spectrum with two resonances at δ 86.57

(dd) and 49.78 (d) ppm corresponding to the =CH trans to phosphorus and nitrogen, respectively.

The mononuclear formulation of **2** has been confirmed by an X-ray diffraction study. A view of the molecular structure is shown in Figure 1 along with selected bond lengths and angles.

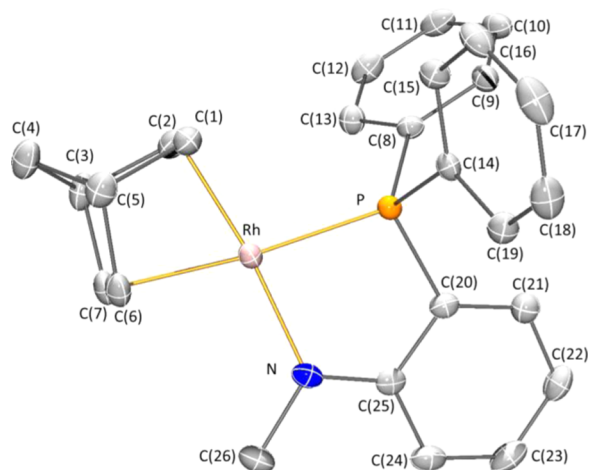


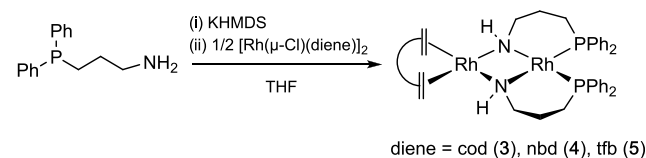
Figure 1. Molecular structure of compound $[\text{Rh}(\text{nbd})\{\text{Ph}_2\text{P}(\text{C}_6\text{H}_4)\text{-NMe}\}]$ (**2**). Hydrogen atoms are omitted for clarity. Selected bond lengths (Å) and angles (deg) are Rh–P 2.2462(8), Rh–N 2.032(2), Rh–Ct(1) 1.992(4), Rh–Ct(2) 2.130(3), P–Rh–N 82.48(8), P–Rh–Ct(1) 103.79(10), P–Rh–Ct(2) 174.03(9), N–Rh–Ct(1) 172.94(13), N–Rh–Ct(2) 103.35(12), and Ct(1)–Rh–Ct(2) 70.46(14). Ct(1) and Ct(2) are the centroids of the C(1)=C(2) and C(6)=C(7) olefinic bonds, respectively.

The molecular structure of **2** exhibits a slightly distorted square-planar metal geometry with the rhodium atom coordinated to the diolefin and to the phosphorus and nitrogen atoms of the chelating phosphino-amido ligand in a $\kappa^2\text{-P}_2\text{N}$ mode. Distortions from the ideal square-planar geometry (characterized by 90° dihedral angles) are due to the small bite angle of the nbd ligand. The observed value in **2** ($70.46(14)^\circ$) nicely agrees with the mean value reported in mononuclear rhodium compounds with tetracoordinated metal atom containing a Rh(nbd) fragment ($70.2(10)^\circ$).²⁴

A planar trigonal geometry is observed in nitrogen atom of the amido group, whose planarity is evidenced by the sum of the bond angles at this atom ($359.7(4)^\circ$). The rhodium–nitrogen bond length deserves special interest. The measured value (2.032(2) Å) is slightly shorter than that reported for the related $[\text{Rh}(\text{cod})\{\text{Ph}_2\text{P}(\text{C}_6\text{H}_4)\text{NMe}\}]$ compound (2.063(1) Å),²³ and both are significantly not longer than those in $[\text{RhCl}(\text{CO})\{\text{Ph}_2\text{P}(\text{C}_6\text{H}_4)\text{NMeH}\}]$ (2.129(2) and 2.140(2) Å for the two independent molecules).²⁵ This feature has been related to the favorable π -interaction of the amido group to the metal atom.²³ The π -donor character of the amido group is also evidenced by the structural differences in the olefin–metal bond. Not only the metal–olefin bond length trans to amido ligand (1.992(4) Å) is shorter than the distance to the olefin trans to the phosphorus atom (2.130(3) Å), but the dissimilarity is also observed in the C=C bond lengths (1.398(5) and 1.364(5) Å for C(1)=C(2) and C(6)=C(7), respectively). The π -donor character of amido group favors the retrodonation of the double bond trans-located, inducing the lengthening of this C=C bond and the contraction of the olefin–metal distance compared to the olefinic bond trans to P atom.

Reaction of the aminophosphine $\text{Ph}_2\text{P}(\text{CH}_2)_3\text{NH}_2$ with complexes $[\text{Rh}(\mu\text{-OMe})(\text{diene})_2]$ afforded red solutions of the dinuclear complexes $[\text{Rh}_2(\text{diene})\{\mu\text{-NH}(\text{CH}_2)_3\text{PPh}_2\}_2]$. However, this procedure does not afford pure compounds, and thus an alternative synthetic approach entailing the efficient deprotonation of the aminophosphine with a strong non-nucleophilic base, such as potassium bis(trimethylsilyl)amide (KHMDS), was explored. The addition of a solution of the salt $\text{K}[\text{Ph}_2\text{P}(\text{CH}_2)_3\text{NH}]$, prepared in situ by reaction of $\text{Ph}_2\text{P}(\text{CH}_2)_3\text{NH}_2$ with KHMDS in tetrahydrofuran, to suspensions of the corresponding compounds $[\text{Rh}(\mu\text{-Cl})(\text{diene})_2]$ in the same solvent gave rise to intensely red-colored solutions from which the dinuclear complexes $[\text{Rh}_2(\text{diene})\{\mu\text{-NH}(\text{CH}_2)_3\text{PPh}_2\}_2]$ (diene = cod, **3**; nbd, **4**; and tfb, **5**) were obtained as red solids in yields around 70% (Scheme 3).

Scheme 3. Synthesis of Dinuclear Rhodium Phosphine-Amido Complexes



Unfortunately, we were unable to prepare the related dinuclear complexes $[\text{Rh}_2(\text{diene})\{\mu\text{-NMe}(\text{CH}_2)_3\text{PPh}_2\}_2]$ featuring bridging 3-(diphenylphosphino)propylmethylamido ligands in pure form following either of the two procedures.

The dinuclear formulation of these compounds has been confirmed with a structural analysis by X-ray diffraction of compound $[\text{Rh}_2(\text{nbd})\{\mu\text{-NH}(\text{CH}_2)_3\text{PPh}_2\}_2]$ (**4**). Complex **4** crystallizes with two crystallographically independent but chemically identical molecules in the unit cell. One of them is depicted in Figure 2 along with selected bond lengths and angles. Although some small differences can be observed between geometrical parameters of the metal coordination sphere of both molecules (see Supporting Information), discussion will be centered in one of them.

The dinuclear framework is supported by two 3-(diphenylphosphino)propylamido ligands exhibiting a $1\kappa^1\text{P}_2:1:2\kappa^2\text{N}$ coordination mode, that is, they are coordinated in a chelating fashion to Rh(1) atom and bridging both metal atoms by means of the coordination to the Rh(2)(nbd) fragment through the amido donor functions. Correspondingly, two phosphino-amido ligands are coordinated to Rh(1) atom with a cis arrangement, with phosphorus–rhodium bond lengths shorter than those reported in complex **2**, reflecting the different trans influence of olefin and amido fragments. Both rhodium atoms exhibit a square-planar coordination. Maximal deviation from an ideal square-planar geometry is found in Rh(2) atom, probably due to the small bite angle of the nbd ligand, as commented in complex **2**.

According to the relative disposition of the substituents of the amido groups and the deviation from planarity of the “RhNRhN” ring, this four-membered ring shows a syn,endo conformation and configuration. The central core is folded around the N–N vector, with a dihedral angle of $63.36(8)^\circ$ between the two metal coordination planes. This disposition leads to a 2.8315(5) Å intermetallic distance, which may suggest the existence of a Rh–Rh bond. This value lies in the upper value of the range of distances observed for other amido-bridged rhodium dimers, where a single bond is thought to

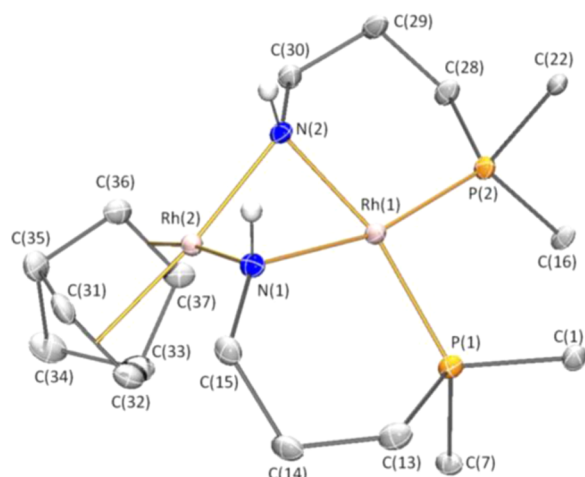


Figure 2. Molecular structure of compound $[\text{Rh}_2(\text{nbd})\{\mu\text{-NH}(\text{CH}_2)_3\text{PPh}_2\}_2]$ (**4**). For clarity, hydrogen atoms (except those of N–H fragments) are omitted and only *ipso*-carbon atoms of phenyl groups are depicted. Selected bond lengths (Å) and angles (deg) are Rh(1)–P(1) 2.2076(10), Rh(1)–P(2) 2.2098(10), Rh(1)–N(1) 2.135(3), Rh(1)–N(2) 2.103(3), Rh(2)–N(1) 2.058(3), Rh(2)–N(2) 2.068(3), Rh(2)–Ct(1) 2.008(4), Rh(2)–Ct(2) 2.003(4), P(1)–Rh(1)–P(2) 97.50(4), P(1)–Rh(1)–N(1) 94.44(9), P(1)–Rh(1)–N(2) 166.99(8), P(2)–Rh(1)–N(1) 166.39(8), P(2)–Rh(1)–N(2) 93.60(9), N(1)–Rh(1)–N(2) 75.42(12), N(1)–Rh(2)–N(2) 77.85(12), N(1)–Rh(2)–Ct(1) 106.7(1), N(1)–Rh(2)–Ct(2) 171.2(1), N(2)–Rh(2)–Ct(1) 173.7(1), N(2)–Rh(2)–Ct(2) 104.8(1), and Ct(1)–Rh(2)–Ct(2) 71.4(2). Ct(1) and Ct(2) are the centroids of the olefinic C(31)–C(32) and C(36)–C(37) bonds, respectively.

exist between metal atoms: intermetallic distance in **2** is longer than those found in $[\{\text{Rh}(\text{PPh}_3)(\text{CO})\text{I}\}_2\{\mu\text{-}(\text{NH})_2\text{C}_{10}\text{H}_6\}]$,²⁶ (2.540(1) Å), $[\text{RhCl}(\text{CO})(\mu\text{-NHC}_6\text{H}_4\text{PPh}_2)_2]$ (2.549(1)),²⁷ $[\text{Cp}^*\text{Rh}(\mu\text{-NHPH})_2]$ (2.6097(9) Å),²⁸ $[\text{Cp}^*\text{Rh}(\mu\text{-NHSO}_2\text{C}_6\text{H}_4\text{Me})_2]$ (2.6004(12) Å),²⁹ and $[\{\text{Rh}(\text{CO})_2\}_2(\mu\text{-}(\text{NH})_2\text{C}_{10}\text{H}_6)]$ (2.810(4) Å)³⁰—dinuclear complexes where the existence of the intermetallic bond has been evoked—comparable to those found in $[\text{Rh}(\text{cod})(\mu\text{-NH}_2)_2]$ (2.7785(3) and 2.8603(3) Å),³¹ $[\text{Rh}(\text{CN}t\text{Bu})_2(\mu\text{-NPh}_2)_2]$ (2.9728(10) Å), and $[\text{Rh}(\text{CN}t\text{Bu})_2(\mu\text{-NHC}_6\text{H}_4\text{Me})_2]$ (2.9899(6) Å) and shorter than that found in $[\text{Rh}(\text{cod})\{\mu\text{-N}(\text{C}_6\text{H}_4\text{Me})_2\}]_2$ (3.2965(11) Å).³² Intermetallic distance and folding of “RhNRhN” central core depends on steric requirements of both substituents of amido groups and of the other ligands coordinated to the metal atoms, and therefore its rationalization is not a trivial statement.

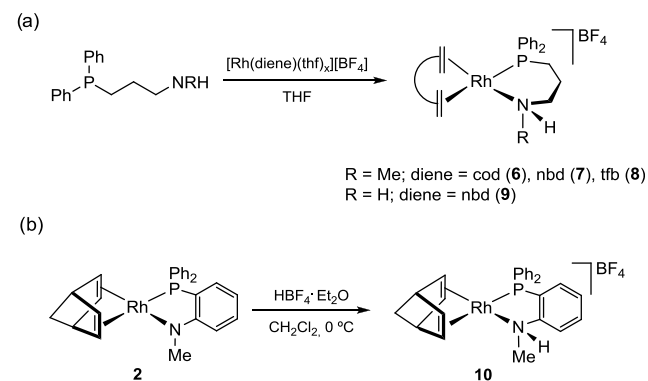
Amido-metal bond lengths are found to be dissimilar, with smaller values found in Rh–N bond trans to olefinic bonds (2.058(3) and 2.068(3) Å) compared to those trans to phosphane (2.135(3) and 2.103(3) Å). This result may point to the π -acceptor character of the olefinic bond, reinforcing both π and σ components of Rh–N bond. This characteristic may also be supported by the good agreement in the geometrical parameters of the coordination of the nbd fragment in compounds **2** and **4**: close values are found in bond length of olefinic bonds (1.398(5) Å in **2**; 1.401(6) and 1.392(6) Å in **4**) and metal–olefin distances (1.992(4) Å in **2**; 2.008(4) and 2.003(4) Å in **4**).

The spectroscopic data for compounds **3**–**5** are in agreement with the solid-state structure of ideal C_2 symmetry found for compound **4**. As an example, the ^1H NMR spectrum of **4** showed two resonances for the olefinic protons = CH of

the nbd ligand at similar chemical shifts, δ 3.49 and 3.44 ppm, corresponding to the nonequivalent exo and endo protons as a consequence of the bent molecular framework. These resonances correlate with two doublet signals at δ 52.94 and 52.48 ppm ($J_{\text{C-Rh}} \approx 10$ Hz) in the ^1H - ^{13}C HSQC NMR spectrum (see the Supporting Information). The nonequivalent CH protons of the nbd ligand gave rise to two signals at δ 3.90 and 3.49 ppm, whereas the equivalent NH protons of the amido groups appeared as a broad signal at δ –0.09 ppm in the ^1H NMR spectrum. In addition, the $^{31}\text{P}\{^1\text{H}\}$ NMR spectra of compounds **3**–**5** showed a doublet resonance in the range $\delta \approx 37$ – 38 ppm with identical coupling constants ($J_{\text{P-Rh}} = 172$ – 173 Hz). The little influence of the electronic character of the diene ligand on the $J_{\text{P-Rh}}$ value is in agreement with the structure of the compounds since the Rh(diene)⁺ fragment is coordinated to the *cis*-amido groups of the structural unit $[\text{Rh}\{\text{NH}(\text{CH}_2)_3\text{PPh}_2\}_2]^-$, which is common for the three compounds and is observed as the doubly protonated fragment, $[\text{Rh}\{\text{Ph}_2\text{P}(\text{CH}_2)_3\text{NH}_2\}_2]^+$, in the ESI+ spectra.

Synthesis of Mononuclear Phosphine-Amino/Diene Rhodium(I) Complexes. The functionalized phosphine $\text{Ph}_2\text{P}(\text{CH}_2)_3\text{NMeH}$ reacts with the solvato $[\text{Rh}(\text{diene})\text{-}(\text{THF})_2]^+$ species, formed in situ by reaction of $[\text{Rh}(\mu\text{-Cl})(\text{diene})_2]$ with AgBF_4 in tetrahydrofuran, to afford yellow suspensions of the cationic complexes $[\text{Rh}(\text{diene})\{\text{Ph}_2\text{P}(\text{CH}_2)_3\text{NHMe}\}][\text{BF}_4]$ (diene = cod, **6**; nbd, **7**; tfb, **8**), which were isolated as yellow solids in 60–70% yields. The related compound $[\text{Rh}(\text{nbd})\{\text{Ph}_2\text{P}(\text{CH}_2)_3\text{NH}_2\}][\text{BF}_4]$ (**9**) has been prepared in 65% yield following the same methodology using the 3-(diphenylphosphino)propan-1-amine ligand (Scheme 4a). The cationic complex $[\text{Rh}(\text{nbd})\{\text{Ph}_2\text{P}(\text{C}_6\text{H}_4\text{-}$

Scheme 4. Synthesis of Cationic Rhodium Phosphino-Amino Complexes



$\text{NHMe}\}][\text{BF}_4]$ (**10**) has been prepared following a different methodology. The protonation of the mononuclear phosphine-amido complex $[\text{Rh}(\text{nbd})\{\text{Ph}_2\text{P}(\text{C}_6\text{H}_4\text{-NMe})\}][\text{BF}_4]$ (**2**) with HBF_4 in dichloromethane at 0 °C gave a yellow solution of compound **10**, which was isolated as a yellow solid in 60% yield (Scheme 4b).

The MALDI-TOF mass spectra of compounds **6**–**10** showed the molecular ion at the expected m/z , and a broad absorption centered at 1055 cm^{-1} was observed in the Fourier-transform infrared spectra for the tetrafluoroborate anion, confirming the ionic character of the complexes. The structure of the compounds is derived from the chelate coordination $\kappa^2\text{P,N}$ of the amino-phosphine ligand to the fragments

$[\text{Rh}(\text{diene})]^+$ that result in the formation of square-planar complexes, which was confirmed by the determination of the molecular structure of compound $[\text{Rh}(\text{nbd})\{\text{Ph}_2\text{P}(\text{CH}_2)_3\text{NHMe}\}][\text{BF}_4]$ (**7**) by X-ray diffraction. The molecular structure of complex **7** is depicted in Figure 3 along with selected bond lengths and angles.

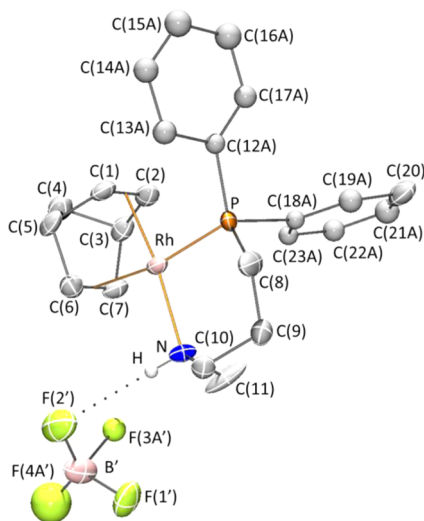


Figure 3. Molecular structure of compound $[\text{Rh}(\text{nbd})\{\text{Ph}_2\text{P}(\text{CH}_2)_3\text{NHMe}\}][\text{BF}_4]$ (**7**). Hydrogen atoms (except that of N–H fragment) have been omitted. Primed atoms are related to unprimed ones through $2 - x, 1 - y, 1 - z$ symmetry operation. Selected bond lengths (Å) and angles (deg) are Rh–P 2.2517(16), Rh–N 2.143(4), Rh–Ct(1) 1.997(5), Rh–Ct(2) 2.138(6), P–Rh–N 92.00(14), P–Rh–Ct(1) 97.88(17), P–Rh–Ct(2) 167.10(17), N–Rh–Ct(1) 170.0(2), N–Rh–Ct(2) 100.0(2), and Ct(1)–Rh–Ct(2) 70.0(2). Ct(1) and Ct(2) are the centroids of the C(1)=C(2) and C(6)=C(7) olefinic bonds, respectively.

Geometrical parameters describing the metal coordination sphere of compound **7** are closely related to those of mononuclear compound **2** (Figure 1). Similar trends are observed in both complexes. Accordingly, differences in trans influence exerted by phosphine and amino fragments in **7** lead to dissimilarities in bond lengths between the metal atom and the olefinic bonds trans to these groups, as commented for compound **2**. No statistical differences are found between Rh–olefinic, Rh–P, and olefinic bond lengths in both compounds.

In fact, main differences between compounds **2** and **7** concern nitrogen atom, which is no longer planar in compound **7**, but exhibit a tetrahedral geometry. The existence of four substituents at the nitrogen atom in compound **7** induces a longer Rh–N bond length (2.143(4) Å in **7**, 2.032(2) Å complex **2**). This difference between amino and amido groups, also reported for $[\text{Rh}(\text{cod})\{\text{Ph}_2\text{P}(\text{C}_6\text{H}_4)\text{NMeH}\}]^+$ (2.148(2) and 2.161(4) Å for the two crystallographically independent molecules) and $[\text{Rh}(\text{cod})\{\text{Ph}_2\text{P}(\text{C}_6\text{H}_4)\text{NMe}\}]$ compounds (2.063(1) Å), has been correlated to the lack of π interaction with the metal atom in the former.

Hydrogen atom of amino fragment in **7** establishes a hydrogen bond with the BF_4^- anion, as shown in Figure 3, characterized by 2.37(9) and 3.172(7) Å H \cdots F and N \cdots F distances, respectively, and a 173(8) $^\circ$ N–H \cdots F angle. As expected, compounds **6–10** are conductors in acetone solutions with molar conductivities Λ_M in the range of 42–57 $\Omega^{-1} \text{ cm}^2 \text{ mol}^{-1}$. These values are somewhat lower than

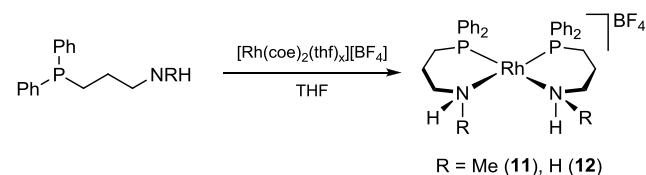
those expected for 1:1 electrolytes in this solvent (80–100 $\Omega^{-1} \text{ cm}^2 \text{ mol}^{-1}$), which suggests the possible formation of ionic pairs by interaction of the BF_4^- with the NH function on the coordinated functionalized phosphine ligand, in agreement with the N–H \cdots F interaction observed in solid-state structure.

The $^{31}\text{P}\{^1\text{H}\}$ NMR spectra of the complexes showed a doublet resonance centered $\delta \approx 17$ –22 ppm for **6–9** and at 37 ppm for **10**, with $J_{\text{P-Rh}}$ in the range of 155–175 Hz. The π -acceptor character of the diene ligand in compounds $[\text{Rh}(\text{diene})\{\text{Ph}_2\text{P}(\text{CH}_2)_3\text{NHMe}\}]^+$ (**6–8**) influences both the chemical shift and the $J_{\text{P-Rh}}$ coupling constant. The increase of the π -acceptor character results in a deshielding of the resonance and an increase of the coupling constant. Unlike compound $[\text{Rh}(\text{nbd})\{\text{Ph}_2\text{P}(\text{CH}_2)_3\text{NH}_2\}][\text{BF}_4]$ (**9**) of C_s symmetry, the rest of the compounds, **6–8** and **10**, are asymmetric, as a consequence of the presence of the methyl substituent on the nitrogen heteroatom. The lack of symmetry is detected in both the ^1H and $^{13}\text{C}\{^1\text{H}\}$ NMR spectra. For example, the ^1H NMR spectrum of $[\text{Rh}(\text{cod})\{\text{Ph}_2\text{P}(\text{CH}_2)_3\text{NHMe}\}][\text{BF}_4]$ (**6**) showed four resonances in the range δ 5.4–2.9 ppm for the nonequivalent =CH protons of the cod ligand. Similarly, the $^{13}\text{C}\{^1\text{H}\}$ NMR spectrum showed two doublet of doublets at δ 108.48 and 104.98 ppm and two doublets at δ 79.05 and 76.10 ppm, corresponding to the =CH trans to the phosphine and amino fragments.

The amine proton of the –NHMe fragment in compounds **6–8** was observed as a broad resonance in the range δ 4.3–3.8 ppm. This resonance appears sometimes overlapped and has been identified with the help of the ^1H – ^1H COSY spectrum due to the small coupling with the methyl group, which was observed as a doublet in the range δ 2.2–2.7 ppm ($J_{\text{H-H}} \approx 6$ Hz). The resonance of the –NH $_2$ group in compound **9** is more shielded (δ 2.86 ppm) while that of the amine proton of the –NHMe fragment in **10** is more deshielded and is observed at δ 6.15 ppm ($J_{\text{H-H}} = 6$ Hz).

Synthesis of Mononuclear Phosphine-Amino Rhodium(II) Complexes. The lability of the cyclooctene (coe) ligand³³ in the solvato species $[\text{Rh}(\text{coe})_2(\text{thf})_2]^+$ with respect to diene ligands has allowed the preparation of cationic compounds containing exclusively functionalized phosphine ligands. The species $[\text{Rh}(\text{coe})_2(\text{thf})_2]^+$ has been prepared in situ by reaction of $[\text{Rh}(\mu\text{-Cl})(\text{coe})_2]_2$ with 2 equiv of AgBF_4 in tetrahydrofuran, followed by elimination of the formed AgCl .³⁴ This species reacts with 2 equiv of the corresponding amino-phosphine, $\text{Ph}_2\text{P}(\text{CH}_2)_3\text{NMeH}$ or $\text{Ph}_2\text{P}(\text{CH}_2)_3\text{NH}_2$, to give orange solutions of compounds $[\text{Rh}\{\text{Ph}_2\text{P}(\text{CH}_2)_3\text{NHMe}\}_2][\text{BF}_4]$ (**11**) and $[\text{Rh}\{\text{Ph}_2\text{P}(\text{CH}_2)_3\text{NH}_2\}_2][\text{BF}_4]$ (**12**), which were isolated as orange solids in 55 and 62% yields, respectively (Scheme 5). These compounds are very sensitive to both oxygen and moisture, and therefore their synthesis has been carried out in a dry box. Unfortunately, compound $[\text{Rh}\{\text{Ph}_2\text{P}(\text{CH}_2)_3\text{NMe}_2\}_2]^+$ bearing the ligand (3-dimethyla-

Scheme 5. Synthesis of Cationic Rhodium bis-Phosphino-Amino Complexes



mino-propyl)diphenylphosphine could not be prepared following this methodology.

Compounds **11** and **12** have been characterized by elemental analysis, mass spectrometry, and multinuclear NMR spectroscopy. The mass spectra (MALDI-TOF) of both compounds showed the molecular ion at m/z 617.2 and 589.1, respectively, which supports their mononuclear formulation. The most notable feature in the ^1H NMR spectra of both compounds is the absence of coordinated cyclooctene and the resonance corresponding to the amine protons of the fragments $-\text{NHMe}$ and $-\text{NH}_2$, which were observed as broad signals at δ 3.82 and 3.57 ppm, respectively. The $^{31}\text{P}\{^1\text{H}\}$ NMR spectra showed a doublet at δ 36.2 and 39.0 ppm ($J_{\text{P-Rh}} = 172\text{--}174$ Hz), indicating that both amino-phosphine ligands are equivalent. Assuming a square-planar structure and a chelate coordination $\kappa^2\text{P,N}$ of the amino-phosphine ligands, two isomers having *cis* or *trans* disposition of both ligands are possible. The structural analysis of compound $[\text{Rh}\{\text{Ph}_2\text{P}(\text{CH}_2)_3\text{NHMe}\}_2][\text{BF}_4]$ (**11**) has been carried out by X-ray diffraction. The molecular structure, shown in Figure 4,

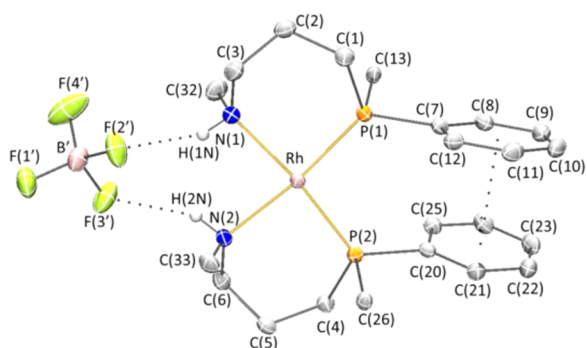


Figure 4. Molecular structure of compound $[\text{Rh}\{\text{Ph}_2\text{P}(\text{CH}_2)_3\text{NHMe}\}_2][\text{BF}_4]$ (**11**). Hydrogen atoms (except those of N–H fragments) are omitted, and only *ipso*-carbon atoms of non-interacting phenyl groups have been depicted. Primed atoms are related to unprimed ones through $x, y, z - 1$ symmetry operation. Selected bond lengths (Å) and angles (deg) are Rh–P(1) 2.2093(6), Rh–P(2) 2.2099(6), Rh–N(1) 2.177(2), Rh–N(2) 2.1794(18), P(1)–Rh–P(2) 98.03(2), P(1)–Rh–N(1) 89.35(5), P(1)–Rh–N(2) 172.40(6), P(2)–Rh–N(1) 172.62(5), P(2)–Rh–N(2) 89.51(6), and N(1)–Rh–N(2) 83.11(7).

confirms the *cis*-arrangement of both 3-(diphenylphosphino)-*N*-methylpropan-1-amine ligands. This mutual placement may be related to the existence of an intramolecular $\pi\cdots\pi$ interaction between two phenyl groups of different phosphines ($\text{G}\cdots\text{G}$ 3.680(3) Å, $\text{Ph}\cdots\text{Ph}$ dihedral angle 10.11(6) $^\circ$), shorter than that found in the analogous $[\text{Rh}\{\text{Ph}_2\text{P}(\text{CH}_2)_3\text{OEt}\}_2]^+$ compound.³⁵

Geometrical parameters of **11** evidence similar features to previously characterized phosphine-amido and phosphine-amino complex compounds. On the one hand, Rh–P bond lengths in **11** are found to be close to those found in complex **4**, where phosphorus atoms are also *trans* to nitrogen ones. On the other hand, amino fragment characteristics in **11** are similar to those of compound **7**. Moreover, hydrogen-bond interactions are also found between both amino groups of compound **11** and BF_4^- anion. These intermolecular interactions (characterized by 2.18(3), 2.951(3), 156(2) and 2.19(3), 2.983(2) and 152(2); $\text{H}\cdots\text{F}$, $\text{N}\cdots\text{F}$ distances and $\text{N}\cdots\text{F}$

$\text{H}\cdots\text{F}$ angles, respectively) lead to the formation of a ring $\text{R}_2^2(8)$ graph set (Figure 4).³⁶

Polymerization of PA by Phosphine-Amido and Phosphine-Amino Rhodium(I) Catalysts. Phosphine-amido complexes, $[\text{Rh}(\text{diene})\{\text{Ph}_2\text{P}(\text{C}_6\text{H}_4)\text{NMe}\}]$ and $[\text{Rh}_2(\text{diene})\{\mu\text{-NH}(\text{CH}_2)_3\text{PPh}_2\}_2]$, and cationic phosphine-amino complexes, $[\text{Rh}(\text{diene})\{\text{Ph}_2\text{P}(\text{CH}_2)_3\text{NHR}\}]^+$ ($\text{R} = \text{H}, \text{Me}$) and $[\text{Rh}(\text{kbd})\{\text{Ph}_2\text{P}(\text{C}_6\text{H}_4)\text{NHMe}\}]^+$, are efficient catalyst precursors for phenylacetylene polymerization. In contrast, complexes $[\text{Rh}\{\text{Ph}_2\text{P}(\text{CH}_2)_3\text{NHR}\}_2]^+$ ($\text{R} = \text{H}, \text{Me}$) were found to be inactive, which reflects the crucial role of a diene ligand for efficient polymerization catalysts design.

PA polymerization reactions by these rhodium(I) catalyst precursors were carried out preferentially in THF at 293 K using a $[\text{PA}]_0/[\text{Rh}]$ ratio of 100, and 1 and 0.5 mol % catalyst loadings for mononuclear and dinuclear precursors, respectively. The PPA polymers were obtained as soluble yellow-orange solids with a plastic-like appearance. The ^1H and $^{13}\text{C}\{^1\text{H}\}$ NMR spectra of the samples have shown a stereoregular structure with a *cis*-*trans*oidal configuration and a *cis*-content higher than 99%.^{37,38} The PPAs have been characterized by size exclusion chromatography (SEC) using light scattering (MALS) and refractive index (DRI) detectors.

The neutral catalysts based on amido-phosphine ligands showed an excellent activity affording PPA of very high molar mass (MM) at high conversion in very short reaction times (15–120 min, Table 1). Among the phosphine-amido

Table 1. Polymerization of PA by Phosphine-Amido Rhodium(I) Catalysts 1–5^a

entry	cat.	solv.	time (min)	conv. (%) ^b	M_w (g mol ⁻¹) ^c	M_w/M_n	IE ^d (%)
1	1	THF	180	44	2.61×10^5 ^f	1.69	2.9
2	1	toluene	150	70	3.72×10^5	2.03	3.9
3	1	CH_2Cl_2	75	100	2.92×10^5 ^f	1.62	5.7
4	2	THF	105	100	2.96×10^6	1.52	0.5
5	3	THF	120	90	2.11×10^5 ^f	1.80	7.8
6 ^e	3	THF	120	70	2.20×10^5 ^f	1.73	5.6
7	4	THF	15	100	1.04×10^6	1.31	1.3
8 ^e	4	THF	15	100	9.49×10^5	1.36	1.5
9	5	THF	15	100	1.19×10^6	1.68	1.4

^aReaction conditions: 293 K, $[\text{PA}]_0 = 0.25$ M, $[\text{PA}]_0/[\text{Rh}] = 100$.

^bDetermined by GC (octane as internal standard). ^cDetermined by SEC-MALS.

^dInitiation efficiency, $\text{IE} = M_{\text{theor}}/M_n \times 100$, where $M_{\text{theor}} = [\text{PA}]_0/[\text{Rh}]_n \times \text{MW}_{\text{PA}} \times \text{polymer yield}$.

^e[DMAP]/[Rh] = 1. ^fBimodal MMD: data for the lower molar mass polymer.

complexes, $[\text{Rh}(\text{diene})\{\text{Ph}_2\text{P}(\text{C}_6\text{H}_4)\text{NMe}\}]$, compound **2** (diene = *nbd*) is considerably more active than **1** (diene = *cod*) in THF affording a PPA with an outstandingly high weight-average molecular weight, M_w , of 2.96×10^6 with a moderate polydispersity index (PDI), M_w/M_n , of 1.52, as a consequence of a very low initiation efficiency, $\text{IE} = 0.52$. Under the same conditions, catalyst **1** gave a 44% of PPA that showed a bimodal molar mass distribution (MMD) profile with a M_w of 2.61×10^5 (entries 1 and 4). As can be seen in the chromatograms of Figure 5, the MALS detector (molar mass-sensitive) shows a shoulder corresponding to a polymer of high molar mass M_w of $\approx 1.96 \times 10^6$, but in small concentration (approximately 3% in weight) as indicated by the DRI detector (concentration-sensitive). The influence of the solvent on the catalyst performance and polymer properties

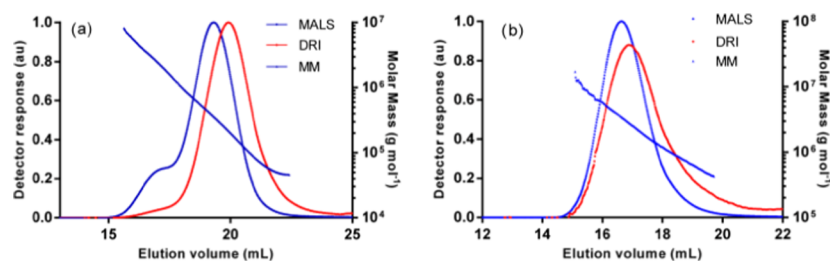


Figure 5. Light scattering (blue) and refractive index (red) chromatograms. MM vs elution volume plots for PPA samples prepared using catalysts: (a) $[\text{Rh}(\text{cod})\{\text{Ph}_2\text{P}(\text{C}_6\text{H}_4)\text{NMe}\}]$ (1) and (b) $[\text{Rh}(\text{nbd})\{\text{Ph}_2\text{P}(\text{C}_6\text{H}_4)\text{NMe}\}]$ (2) in THF.

has been studied with catalyst **1**. The polymerization in dichloromethane is much faster (100% conversion in 75 min) also giving a polymer with a bimodal MMD profile and a M_w of 2.92×10^5 (entry 3). In contrast, a polymer with a unimodal distribution and a higher M_w of 3.72×10^5 was obtained in toluene, although only a slight improvement in the activity was attained (entry 2). Interestingly, the related rhodium(I) complex $[\text{Rh}(\text{cod})(\text{Ph}_2\text{PCH}_2\text{CH}_2\text{NTs})]$ ($\text{Ts} = \text{SO}_2\text{C}_6\text{H}_4\text{-}p\text{-Me}$) featuring a phosphinosulfonamido ligand polymerized PA (1 mol % catalyst loading, 40–74% in 2 h) in a range of solvents of different polarities (CH_2Cl_2 , benzene, and THF) affording PPAs with unimodal gel permeation chromatography (GPC) profiles with much lower molecular weights, M_w , in the range of $(2.86\text{--}6.32) \times 10^4$ and wider molecular weight distribution ($\text{PDI} > 2.2$).²¹

The dinuclear amido-phosphine $[\text{Rh}_2(\text{diene})\{\mu\text{-NH}(\text{CH}_2)_3\text{PPh}_2\}_2]$ precursors showed a remarkable catalytic activity in PA polymerization. Catalysts **4** (diene = nbd) and **5** (diene = tfb) afforded complete PA conversion in only 15 min. However, catalyst **3** (diene = cod) required 120 min to reach a 90% conversion (entries 5, 7, and 9). The MMs of the PPAs obtained with catalysts **4** and **5** are very high, M_w of 1.04×10^6 and 1.19×10^6 , with initiation efficiencies of 1.3 and 1.4%, respectively, and PDIs of 1.31 and 1.68, respectively. In this respect, the low PDI value of the PPA prepared with **4** is remarkable. On the other hand, the PPA produced by **3** showed a lower MM, M_w of 2.11×10^5 , a bimodal MMD, and a greater polydispersity ($\text{PDI} = 1.80$). As can be seen in the chromatograms of Figure 6, the DRI chromatogram (concentration-sensitive) for the PPA obtained with catalyst **3** shows a shoulder corresponding to a polymer in low concentration (ca. 3% in weight) of high molar mass, M_w of $\approx 2.43 \times 10^6$, as indicated by the MALS detector (molar mass-sensitive). The described results evidence that catalysts having nbd or tfb as diene ligand are much more active than the cod counterpart,

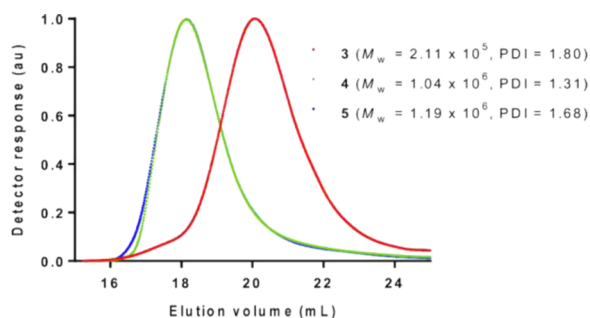


Figure 6. Refractive index chromatograms (DRI) for PPA samples prepared with catalysts **3** (red), **4** (green), and **5** (blue) in THF.

which is in agreement with the results reported by Masuda et al.^{39,40} Likely, the high π -acidity of nbd and tfb results in the reduction of the electronic density at the rhodium center enhancing its electrophilic character, thereby facilitating the coordination of the monomer. Interestingly, the log–log plot of the radius of gyration (r_g) vs the molar mass (MM) for the polymers obtained with catalysts **1–5** in THF showed a linear trend, which is characteristic of a linear polymer (see the Supporting Information).

PA polymerization studies by rhodium(I) catalysts have shown that the addition of a base as co-catalyst, as for example 4-(dimethylamino)pyridine (DMAP) or *i*-PrNH₂, usually leads to an improvement of the catalyst performance as a result of an increase of the initiation efficiency^{41–43} or the inhibition of catalyst deactivation pathways.⁴⁴ With the aim to increase the initiation efficiency and to reduce the polydispersity of the PPA, the influence of the co-catalyst 4-(dimethylamino)pyridine (DMAP) in the polymerization of PA by catalysts **3** (diene = cod) and **4** (diene = nbd) has been studied using a $[\text{DMAP}]/[\text{Rh}]$ ratio of 1. The presence of an external base such as DMAP does not influence the catalytic activity in the case of catalyst **4**, although it is slightly reduced with **3**. Regarding the polymer properties, both catalysts exhibited opposite tendencies. While in the case of **4** the addition of DMAP produces a slight increase of the polydispersity and the initiation efficiency, a decrease of both parameters was observed with catalyst **3** (entries 6 and 8). Additionally, the catalytic system **3**/DMAP produces a PPA with a more pronounced bimodal character. Therefore, the addition of an external base does not have the expected positive effect on the polymerization reaction.

The cationic complexes $[\text{Rh}(\text{diene})\{\text{Ph}_2\text{P}(\text{CH}_2)_3\text{NHR}\}]^+$ ($\text{R} = \text{H}, \text{Me}$) and $[\text{Rh}(\text{nbd})\{\text{Ph}_2\text{P}(\text{C}_6\text{H}_4)\text{NHMe}\}]^+$ efficiently catalyzed the polymerization of PA, although, in general, they are less active than the corresponding amido complexes (Table 2). The most active catalysts are those containing strong π -acceptor diene ligands such as nbd or tfb. In the series of complexes $[\text{Rh}(\text{diene})\{\text{Ph}_2\text{P}(\text{CH}_2)_3\text{NHMe}\}]\text{BF}_4$ (**6–8**), a conversion of $\geq 75\%$ was reached in 90 min with catalysts **7** (nbd) and **8** (tfb), while a 55% conversion was attained with **6** (cod) after 120 min. In addition, a high-molecular-weight stereoregular polymer was obtained with catalysts **7** (nbd) and **8** (tfb), M_w of 1.86×10^6 ($\text{IE} = 0.62$) and 1.08×10^6 ($\text{IE} = 1.32$), respectively, with moderate polydispersities ($\text{PDI} \approx 1.7$). In contrast, the PPA produced by **6** (cod) has a much lower MM, M_w of 2.93×10^5 ($\text{IE} = 3.60$) and a wider MMD ($\text{PDI} = 1.85$) (Figure 7).

The nature of the bidentate phosphine ligand also exerts a significant influence on the catalyst performance. The cationic complexes $[\text{Rh}(\text{nbd})\{\text{Ph}_2\text{P}(\text{CH}_2)_3\text{NH}_2\}][\text{BF}_4]$ (**9**) and $[\text{Rh}(\text{nbd})\{\text{Ph}_2\text{P}(\text{C}_6\text{H}_4)\text{NHMe}\}][\text{BF}_4]$ (**10**) are more active than **7**

Table 2. Polymerization of PA by Phosphine-Amino Rh(I) Complexes 6–10 and $[\text{Rh}(\text{diene})\text{L}]^+$, $\text{L} = \{\text{Ph}_2\text{P}(\text{CH}_2)_3\text{NMe}_2\}^a$

entry	catalyst	time (min)	conv. (%) ^b	M_w (g mol ⁻¹) ^c	M_w/M_n	IE (%) ^d
1	6	120	55	2.93×10^5	1.85	3.6
2	7	90	75	1.89×10^6	1.67	0.6
3	8	90	80	1.08×10^6	1.74	1.3
4	9	90	100	2.39×10^6	1.59	0.7
5	10	90	100	2.81×10^6	1.86	0.7
6 ^e	$[\text{Rh}(\text{cod})\text{L}]^+$	120	100	2.38×10^5	1.79	7.7
7 ^e	$[\text{Rh}(\text{nbd})\text{L}]^+$	60	100	2.18×10^6	2.00	0.9
8 ^e	$[\text{Rh}(\text{tfb})\text{L}]^+$	60	100	3.25×10^6	2.08	0.7

^aReaction conditions: THF, 293 K, $[\text{PA}]_0 = 0.25 \text{ M}$, $[\text{PA}]_0/[\text{Rh}] = 100$. ^bDetermined by GC (octane as internal standard). ^cDetermined by SEC-MALS. ^dInitiation efficiency, $\text{IE} = M_{\text{theor}}/M_n \times 100$, where $M_{\text{theor}} = [\text{PA}]_0/[\text{Rh}] \times \text{MW}_{\text{PA}} \times \text{polymer yield}$. ^eRef 10.

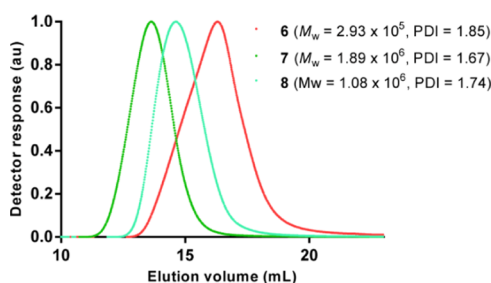


Figure 7. Light scattering chromatograms (MALS) for PPA samples prepared with catalysts 6 (red), 7 (green), and 8 (blue) in THF.

(nbd), reaching full PA conversion in 90 min. On the other hand, the MMs of the PPAs obtained with both catalysts, M_w of 2.39×10^6 and 2.81×10^6 , respectively, are higher than that obtained with 7 ($M_w = 1.89 \times 10^6$), all of them with moderate polydispersities (PDI in the range 1.6–1.9) and initiation efficiencies around 0.6–0.7%.

The cationic catalysts $[\text{Rh}(\text{diene})\{\text{Ph}_2\text{P}(\text{CH}_2)_3\text{NMe}_2\}]^+$ having the functionalized phosphine ligand 3-(diphenylphosphine)-*N,N*-dimethylpropan-1-amine are more active than the corresponding complexes $[\text{Rh}(\text{diene})\{\text{Ph}_2\text{P}(\text{CH}_2)_3\text{NHMe}\}]^+$ (6–8) with the same diene ligand (cod, nbd, or tfb) (Table 2).⁹ In general, the catalysts featuring the $-\text{NMe}_2$ hemilabile fragment provided PPAs of higher MM than the corresponding complexes with the $-\text{NHMe}$ functional group, except for catalyst 6 (cod). Interestingly, catalyst $[\text{Rh}(\text{tfb})\{\text{Ph}_2\text{P}(\text{CH}_2)_3\text{NMe}_2\}]^+$ affords a PPA with a M_w of 3.25×10^6 , 3 times greater than that obtained with 8 (tfb).

The influence of the substitution on the amino fragment can be studied in the series of compounds $[\text{Rh}(\text{nbd})\{\text{Ph}_2\text{P}(\text{CH}_2)_3\text{NMe}_2\}]^+$, $[\text{Rh}(\text{nbd})\{\text{Ph}_2\text{P}(\text{CH}_2)_3\text{NHMe}\}]^+$ (7), and $[\text{Rh}(\text{nbd})\{\text{Ph}_2\text{P}(\text{CH}_2)_3\text{NH}_2\}]^+$ (9), which possess nbd as diene ligand, and $-\text{NMe}_2$, $-\text{NHMe}$, and $-\text{NH}_2$ hemilabile fragments, respectively. If the following, $\text{p}K_a$ values are taken as a reference: NMe_3 (9.76), NHMe_2 (10.64), and NH_2Me (10.62);⁴⁵ the basicity of the fragments $-\text{NHMe}$ and $-\text{NH}_2$ should be comparable to and greater than that of $-\text{NMe}_2$. However, the initiation efficiency of $[\text{Rh}(\text{nbd})\{\text{Ph}_2\text{P}(\text{CH}_2)_3\text{NMe}_2\}]^+$ (EI = 0.9) is higher than those of 7 (EI = 0.6) and 9 (EI = 0.7).

The slightly higher initiation efficiency of the catalysts having a functionalized phosphine ligand with a $-\text{NMe}_2$ fragment (except for diene = cod; Table 2) does not show a direct correlation with the basicity. In principle, the greater basicity of the hemilabile fragment should facilitate the deprotonation of coordinated PA and the formation of the corresponding alkynyl species likely responsible of the initiation process. However, for this to happen, the uncoordination of the hemilabile fragment is required, which should be easier for the catalysts with the $-\text{NMe}_2$ fragment due to the steric influence of both methyl groups. In fact, the Rh–N bond distances found in compounds $[\text{Rh}(\text{diene})\{\text{Ph}_2\text{P}(\text{CH}_2)_3\text{NMe}_2\}]\text{BF}_4$, 2.262(3) Å (cod) and 2.190(4) Å (tfb), are longer than the distance of 2.143(4) Å found in $[\text{Rh}(\text{nbd})\{\text{Ph}_2\text{P}(\text{CH}_2)_3\text{NHMe}\}]\text{BF}_4$ (7).

The analysis of the PPAs produced using complexes $[\text{Rh}(\text{diene})\{\text{Ph}_2\text{P}(\text{CH}_2)_3\text{NMe}_2\}]\text{BF}_4$ by SEC-MALS or A4F-MALS (A4F, asymmetric flow field flow fractionation) showed that the samples contain a mixture of linear and branched polymers.¹⁰ The levels of branching are consistent with either terminal branching through copolymerization of unsaturated macromonomer or chain transfer to polymer, where the branched species are less reactive than the linear chains toward further polymerization. The analysis by SEC-MALS of the PPAs obtained with catalysts $[\text{Rh}(\text{diene})\{\text{Ph}_2\text{P}(\text{CH}_2)_3\text{NHMe}\}]^+$ (6–8) evidenced the presence of branched PPA only in the sample obtained with catalyst 6 (cod).¹⁰

The light scattering and refractive index chromatograms of a PPA sample produced with catalyst 6 (cod) are shown in Figure 8a. The light scattering detector revealed a detectable increase in MM on the high-MM region of the main peak, which is consistent with the presence of branched material. The log–log plot of r_g vs MM revealed significant deviations from linear behavior in the high MM region also consistent with branching (Figure 8b). Interaction of the conjugated PPA material with the column packing is reflected in both the tailing intensity on the light scattering detector beyond the low-MM

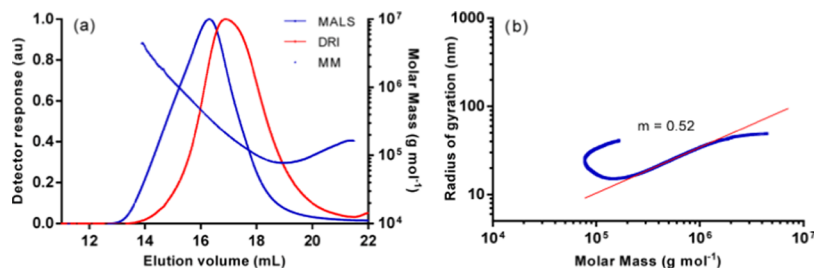


Figure 8. (a) Light scattering (blue) and refractive index (red) chromatograms, MM vs elution volume plot for a PPA sample prepared using catalyst $[\text{Rh}(\text{cod})\{\text{Ph}_2\text{P}(\text{CH}_2)_3\text{NHMe}\}]\text{BF}_4$ (6) in THF. (b) Log–log plot of the radius of gyration (r_g) vs MM.

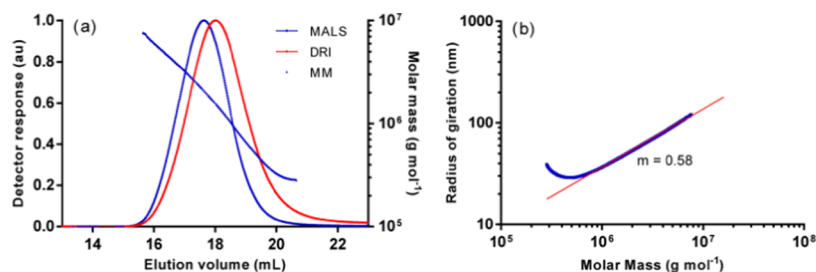


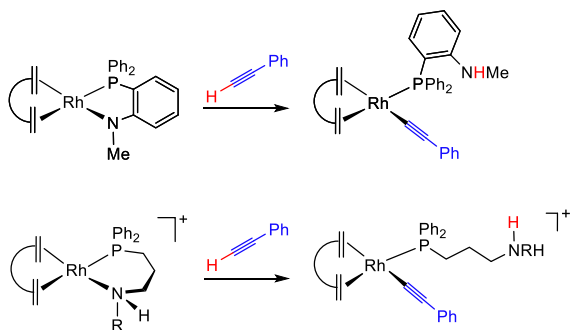
Figure 9. (a) Light scattering (blue) and refractive index (red) chromatograms, MM vs elution volume plot for a PPA sample prepared using catalyst $[\text{Rh}(\text{nb})\{\text{Ph}_2\text{P}(\text{CH}_2)_3\text{NHMe}\}][\text{BF}_4]$ (**7**) in THF. (b) Log–log plot of the radius of gyration (r_g) vs MM.

exclusion limit of the column set and the quirky shape of the conformation plot in the low-MM region.

In contrast, the PPA sample produced with catalyst **7** (**nb**) exhibited a very different behavior as it appeared to be linear over the elution volume ranges, where both MALS and DRI detectors have detectable intensity (Figure 9a). This fact was further confirmed in the log–log plot of r_g vs MM exhibiting a linear relationship in the high-molar-mass region (Figure 9b). The slopes of the linear part of the conformation plots are 0.52 (**6**) and 0.58 (**7**) in THF. The deviation of the expected value of ca. 0.58 for a linear polymer reflects the complex behavior of PPA in diluted solutions due to solvent–polymer and polymer–polymer interaction changes as well as σ -trans to σ -cis isomerization process.⁴⁶ Catalyst precursors $[\text{Rh}(\text{tfb})\{\text{Ph}_2\text{P}(\text{CH}_2)_3\text{NHMe}\}][\text{BF}_4]$ (**8**) and $[\text{Rh}(\text{nb})\{\text{Ph}_2\text{P}(\text{CH}_2)_3\text{NH}_2\}][\text{BF}_4]$ (**9**) also afforded linear PPAs, as evidenced by the linear conformation plots. However, the conformation plot of the PPA obtained with catalyst $[\text{Rh}(\text{nb})\{\text{Ph}_2\text{P}(\text{C}_6\text{H}_4)\text{NHMe}\}][\text{BF}_4]$ (**10**) showed a deviation from linearity in the high-molar-mass region consistent with the presence of branched material (see the Supporting Information).¹⁰

Mechanistic Considerations. Mechanistic investigations on PA polymerization by catalyst precursor $[\text{Rh}(\text{cod})\{\text{Ph}_2\text{P}(\text{CH}_2)_3\text{NMe}_2\}]^+$ allowed us to identify key Rh-alkynyl species formed by intramolecular proton transfer from a η^2 -alkyne ligand to the uncoordinated NMe₂ group.⁹ Based on this finding, PA activation by the related mononuclear phosphino-amino $[\text{Rh}(\text{diene})\{\text{Ph}_2\text{P}(\text{CH}_2)_3\text{NHR}\}]^+$ complexes should afford a cationic species like $[\text{Rh}(\text{diene})\{\text{Ph}_2\text{P}(\text{CH}_2)_3\text{NH}_2\text{R}\}(\text{C}\equiv\text{C-Ph})]^+$. In the same way, a neutral alkynyl species $[\text{Rh}(\text{diene})\{\text{Ph}_2\text{P}(\text{C}_6\text{H}_4)\text{NHMe}\}(\text{C}\equiv\text{C-Ph})]$ should be formed in the case of the mononuclear phosphino-amido complexes $[\text{Rh}(\text{diene})\{\text{Ph}_2\text{P}(\text{C}_6\text{H}_4)\text{NMe}\}]$ (Scheme 6). These alkynyl intermediates could be involved in the initiation

Scheme 6. PA Activation by Mononuclear Phosphino-Amido and Phosphino-Amino Rhodium(I) Complexes

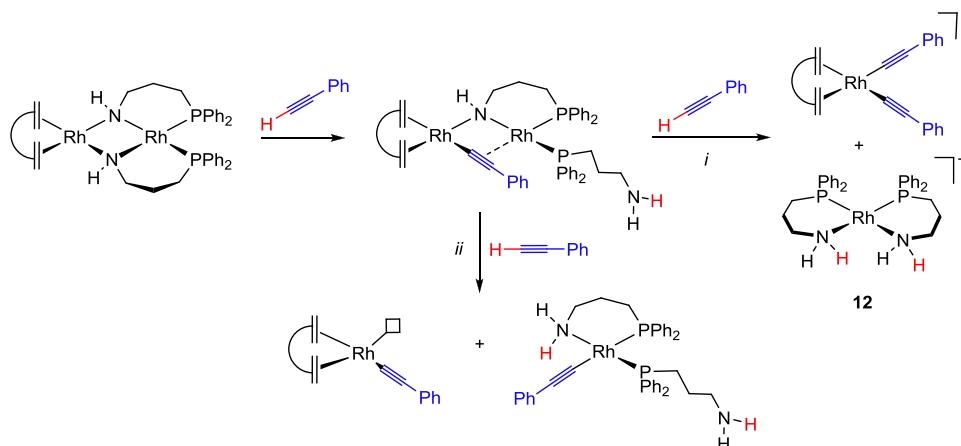
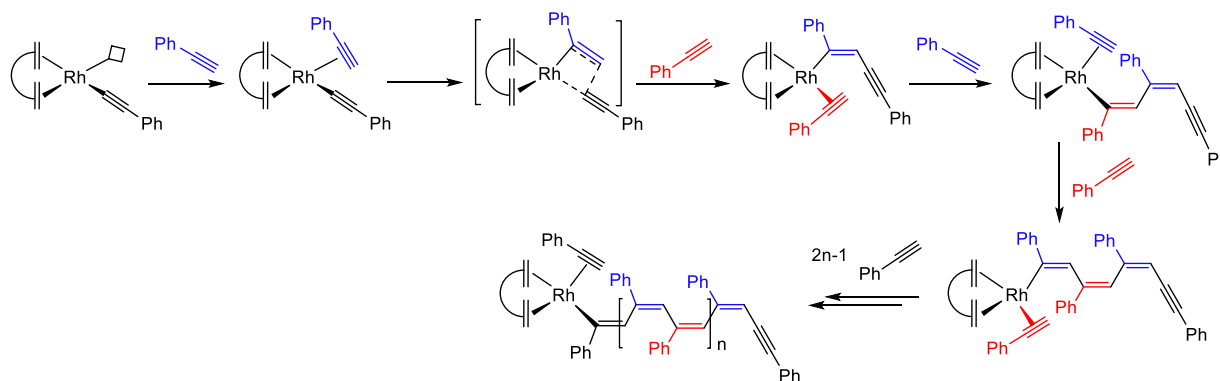


step that likely entails the PA insertion into the Rh-alkynyl bond to afford a stable rhodium-vinyl species responsible for the propagation step by successive PA coordination-insertion reactions.

The proposed scheme for PA activation by catalysts $[\text{Rh}(\text{nb})\{\text{Ph}_2\text{P}(\text{C}_6\text{H}_4)\text{NMe}\}]$ (**2**) and $[\text{Rh}(\text{nb})\{\text{Ph}_2\text{P}(\text{C}_6\text{H}_4)\text{NHMe}\}]^+$ (**10**) should afford closely related active alkynyl species, $[\text{Rh}(\text{nb})\{\text{Ph}_2\text{P}(\text{C}_6\text{H}_4)\text{NHMe}\}(\text{C}\equiv\text{C-Ph})]$ and $[\text{Rh}(\text{nb})\{\text{Ph}_2\text{P}(\text{C}_6\text{H}_4)\text{NH}_2\text{Me}\}(\text{C}\equiv\text{C-Ph})]^+$, respectively. Both species, which only differ in the charge due to the presence of the ammonium group in the later, exhibited similar catalytic activity and IE, which suggests that the charge of the propagating Rh-vinyl species does not have an impact on the catalytic performance.

The formation of alkynyl species from the dinuclear phosphino-amido complexes $[\text{Rh}_2(\text{diene})\{\mu\text{-NH}(\text{CH}_2)_3\text{PPh}_2\}_2]$ with the ability to initiate the polymerization process can take place through different pathways (Scheme 7). Protonation of the nitrogen atom of one of the bridging amido ligands by $\text{PhC}\equiv\text{CH}$ should result in the formation of a Rh-alkynyl bond and an amino-phosphine ligand $\kappa^1\text{P}$ coordinated. Most probably, the alkynyl ligand facilitates the stabilization of the dinuclear unsaturated species through a η^2 interaction. This intermediate species could react further with $\text{PhC}\equiv\text{CH}$ by protonation of the remaining bridging amido ligand resulting in the fragmentation of the dinuclear structure. At this point, the reaction can evolve in two different ways. The new alkynyl ligand can coordinate to the rhodium center bearing the alkynyl ligand, which would give rise to an anionic bis-alkynyl rhodium complex $[\text{Rh}(\text{diene})(\text{C}\equiv\text{C-Ph})_2]^-$ and the cationic compound $[\text{Rh}\{\text{Ph}_2\text{P}(\text{CH}_2)_3\text{NH}_2\}_2]^+$ (**12**) by coordination of the amino fragments of both parent amido ligands (pathway i). Although several bis-alkynyl rhodium(III) complexes have been reported,^{47–49} related rhodium(I) anionic complexes have not been yet described. Although bis-alkynyl species $[\text{Rh}(\text{diene})(\text{C}\equiv\text{C-Ph})_2]^-$ have the potential for PA polymerization, their anionic character should disfavor the coordination of PA, which would not be compatible with the very high catalytic activity exhibited by the dinuclear phosphino-amido complexes. Unfortunately, the attempts to prepare the anionic compound $\text{Li}[\text{Rh}(\text{cod})(\text{C}\equiv\text{C-Ph})_2]$ have been unsuccessful. On the other hand, we have shown that compound **12** is not active in PA polymerization, which practically rules out pathway i as a possible activation mode.

However, if the new alkynyl ligand coordinates to the second rhodium center, two different mononuclear neutral alkynyl species could be formed (pathway ii). The first one is a $14e^-$ unsaturated species that can be stabilized by a molecule of solvent or a π -alkyne ligand, which may be competent for PA polymerization. The second species is a square-planar alkynyl

Scheme 7. Possible Modes of PA Activation by Dinuclear Amido-Phosphine Complexes $[\text{Rh}_2(\text{diene})\{\mu\text{-NH}(\text{CH}_2)_3\text{PPh}_2\}_2]$ Scheme 8. Plausible Mechanism for the Polymerization of PA by $[\text{Rh}(\text{diene})(\text{C}\equiv\text{C-Ph})(\text{PA})]$ 

complex having two amino-phosphine ligands $\kappa^1\text{-P}$ and $\kappa^2\text{-P,N}$ coordinated, which, in principle, should not have the capacity to polymerize PA since it lacks a diene ligand. It is worth noting that the presence of a diene ligand in the catalysts induces a significant backdonation from filled 4d orbitals of rhodium to the lowest unoccupied molecular orbital of the diene ligand, thereby facilitating the PA coordination to the rhodium center.^{40,50}

We suggest that the labile species $[\text{Rh}(\text{diene})(\text{C}\equiv\text{C-Ph})\text{L}]$ ($\text{L} = \text{PA}, \text{THF}$) could be responsible for the outstanding PA polymerization catalytic activity exhibited by the dinuclear phosphino-amido complexes $[\text{Rh}_2(\text{diene})\{\mu\text{-NH}(\text{CH}_2)_3\text{PPh}_2\}_2]$. Insertion of the coordinated PA into the Rh-alkynyl bond of $[\text{Rh}(\text{diene})(\text{C}\equiv\text{C-Ph})(\text{PA})]$, through a four-membered ring transition state, gives a $14e^-$ vinyl species, in which the facile coordination of a second PA molecule at the vacant site followed by cis-insertion into the Rh-vinyl bond with 2,1-regioselectivity initiates the propagation step. After that, successive PA coordination-insertion reactions give PPA having $-\text{C}\equiv\text{C-Ph}$ and a Rh residue at the chain ends (Scheme 8). Theoretical studies by Morokuma et al.⁵¹ with catalyst $[\text{Rh}(\text{nbd})(\text{C}\equiv\text{C-Ph})(\text{PA})]$ have shown that the energy barrier for the PA insertion into the Rh-alkynyl bond (initiation step) is almost 4 kcal mol^{-1} higher than the barrier for the insertion into the Rh-vinyl bond (propagation step), which is in agreement with the low initiation efficiency observed for 4, 2.6% considering that only one of the rhodium atoms of the dinuclear precursor becomes an active species. On the one hand, related active species could also be involved in the PA polymerization by the widely used catalyst precursor

$[(\eta^6\text{-C}_6\text{H}_5\text{-BPh}_3)\text{Rh}(\text{nbd})]$, which show a catalytic performance comparable to 4.⁵²

Further support for this proposal comes from the studies by Shiotsuki and Sanda et al. on PA polymerization by catalyst $[\{\text{nbd}(\text{CH}_2)_4\text{-PPh}_2\}\text{RhR}]$ ($\text{R} = \text{triphenylvinyl}$), which possesses a diene-phosphine ligand coordinated in a $\eta^4, \kappa\text{-P}$ fashion and a triphenylvinyl ligand.⁵³ Theoretical studies have shown that the initiation of the polymerization process requires the uncoordination of the phosphine fragment to generate a center of $14e^-$ with a coordinating vacancy that initiates the polymerization process by PA coordination and subsequent insertion in the Rh-vinyl bond.

CONCLUSIONS

The new amino-functionalized phosphines $\text{Ph}_2\text{P}(\text{CH}_2)_3\text{NMeH}$ and $\text{Ph}_2\text{P}(\text{CH}_2)_3\text{NH}_2$ have been prepared by photochemical hydrophosphination of the corresponding functionalized allyl derivatives. Reaction of the rigid amino-phosphine $\text{Ph}_2\text{P}(\text{C}_6\text{H}_4)\text{NMeH}$ with complexes $[\text{Rh}(\mu\text{-OMe})(\text{diene})_2]$ affords square-planar mononuclear phosphine-anilido $[\text{Rh}(\text{diene})\{\text{Ph}_2\text{P}(\text{C}_6\text{H}_4)\text{NMe}\}]$ (diene = cod, nbd) complexes. In sharp contrast, the flexible amino-phosphine $\text{Ph}_2\text{P}(\text{CH}_2)_3\text{NH}_2$ gives unusual dinuclear complexes $[\text{Rh}_2(\text{diene})\{\mu\text{-NH}(\text{CH}_2)_3\text{PPh}_2\}_2]$ (diene = cod, nbd, tfb) featuring bridging 3-(diphenylphosphino)propylmethylamido ligands. These complexes are obtained in good yield by in situ deprotonation of the amino-phosphine followed by reaction with the corresponding $[\{\text{Rh}(\mu\text{-Cl})(\text{diene})\}_2]$ dinuclear complexes. The cationic mononuclear $[\text{Rh}(\text{diene})\{\text{Ph}_2\text{P}(\text{CH}_2)_3\text{NHR}\}]^+$ ($\text{R} =$

H, Me) complexes have been prepared by reaction of the solvato $[\text{Rh}(\text{diene})(\text{THF})_2]^+$ species with the corresponding amino-phosphine. However, reaction with the cyclooctene solvato $[\text{Rh}(\text{coe})_2(\text{thf})_2]^+$ species affords $[\text{Rh}\{\text{Ph}_2\text{P}(\text{CH}_2)_3\text{NHR}\}_2]^+$ (R = H, Me) complexes featuring a *cis*-arrangement of both amino-phosphine ligands.

The dinuclear phosphino-amido $[\text{Rh}_2(\text{diene})\{\mu\text{-NH}(\text{CH}_2)_3\text{PPh}_2\}_2]$ complexes show a remarkable catalytic activity in PA polymerization. The most active catalysts are those containing strong π -acceptor diene ligands such as nbd or tfb affording stereoregular PPAs of very high molecular weights, M_w up to $\approx 1.2 \times 10^6$, and moderate PDIs. The mononuclear phosphino-anilido $[\text{Rh}(\text{diene})\{\text{Ph}_2\text{P}(\text{C}_6\text{H}_4)\text{NMe}\}]$ complexes are in general less active than the dinuclear complexes bearing the same diene ligand. Noteworthy, a PPA with a M_w of about 3.0×10^6 has been obtained with catalyst $[\text{Rh}(\text{nbd})\{\text{Ph}_2\text{P}(\text{C}_6\text{H}_4)\text{NMe}\}]$ as a consequence of a very low initiation efficiency. The cationic complexes $[\text{Rh}(\text{diene})\{\text{Ph}_2\text{P}(\text{CH}_2)_3\text{NHR}\}]^+$ (R = H, Me) and $[\text{Rh}(\text{nbd})\{\text{Ph}_2\text{P}(\text{C}_6\text{H}_4)\text{NHMe}\}]^+$ are also efficient PA polymerization catalysts, although, in general, they are less active than the corresponding amido complexes. The nature of the bidentate phosphine ligand also influences the catalyst performance of cationic complexes. Catalyst precursors $[\text{Rh}(\text{nbd})\{\text{Ph}_2\text{P}(\text{CH}_2)_3\text{NH}_2\}]^+$ and $[\text{Rh}(\text{nbd})\{\text{Ph}_2\text{P}(\text{C}_6\text{H}_4)\text{NHMe}\}]^+$ exhibit a comparable catalytic activity and are more active than $[\text{Rh}(\text{nbd})\{\text{Ph}_2\text{P}(\text{CH}_2)_3\text{NHMe}\}]^+$ affording PPAs of M_w in the range of $(2.4\text{--}2.8) \times 10^6$ with moderate polydispersities. However, complexes $[\text{Rh}\{\text{Ph}_2\text{P}(\text{CH}_2)_3\text{NHR}\}_2]^+$ (R = H, Me) without a diene ligand are inactive, which reflects the decisive role of a diene ligand in the catalysts. The analysis by SEC-MALS of the PPAs produced by the phosphino-amido and phosphino-amino rhodium(I) catalyst precursors evidences the formation of linear PPAs. However, the conformation plots for the PPAs obtained with $[\text{Rh}(\text{cod})\{\text{Ph}_2\text{P}(\text{CH}_2)_3\text{NHMe}\}]^+$ and $[\text{Rh}(\text{nbd})\{\text{Ph}_2\text{P}(\text{C}_6\text{H}_4)\text{NHMe}\}]^+$ are consistent with the presence of branched material.

The outstanding catalytic activity of dinuclear phosphino-amido $[\text{Rh}_2(\text{diene})\{\mu\text{-NH}(\text{CH}_2)_3\text{PPh}_2\}_2]$ (diene = nbd, tfb) complexes is a consequence of the mode of activation of PA that likely results in the formation of an unsaturated alkynyl species $[\text{Rh}(\text{diene})(\text{C}\equiv\text{C-Ph})\text{L}]$ (L = PA, THF) stabilized by a molecule of solvent or a π -alkyne ligand, which may be competent for PA polymerization.

EXPERIMENTAL SECTION

Synthesis. All experiments were carried out under an atmosphere of argon using Schlenk techniques or glovebox. Solvents were distilled immediately prior to use from the appropriate drying agents or obtained from a solvent purification system (Innovative Technologies). CDCl_3 , CD_2Cl_2 , D_6D_6 , and $\text{THF-}d_8$ (Euriso-top) were dried using activated molecular sieves. The starting materials $[\text{Rh}(\mu\text{-Cl})(\text{diene})_2]$ (diene = cod,⁵⁴ nbd,⁵⁵ tfbb⁵⁶) and $[\text{Rh}(\mu\text{-OMe})(\text{nbd})_2]$ ⁵⁷ were prepared as described in the literature. The functionalized phosphine $\text{Ph}_2\text{P}(\text{C}_6\text{H}_4)\text{NHMe}$ ²⁵ and compound $[\text{Rh}(\text{cod})\{\text{Ph}_2\text{P}(\text{C}_6\text{H}_4)\text{NMe}\}]$ (**1**)²³ were prepared following the reported methods. Diphenylphosphine and phenylacetylene were purchased from Aldrich. Phenylacetylene was purified by vacuum distillation from CaH_2 and stored over molecular sieves.

Scientific Equipment. C, H, and N analyses were carried out in a PerkinElmer 2400 Series II CHNS/O analyzer. ^1H and $^{13}\text{C}\{^1\text{H}\}$ NMR spectra were recorded on a Bruker Avance 300 (300.1276 and 75.4792 MHz) or Bruker Avance 400 (400.1625 and 100.6127 MHz) spectrometers. NMR chemical shifts are reported in ppm relative to tetramethylsilane and referenced to partially deuterated solvent

resonances. Coupling constants (J) are given in hertz. Spectral assignments were achieved by a combination of $^1\text{H-}^1\text{H}$ COSY, $^{13}\text{C}\{^1\text{H}\}$ -APT, and $^1\text{H-}^{13}\text{C}$ HSQC experiments. Electrospray mass spectra (ESI-MS) were recorded on a Bruker MicroTOF-Q using sodium formate as the reference. MALDI-TOF mass spectra were obtained on a Bruker MICROFLEX spectrometer using DCTB, *trans*-2-[3-(4-*tert*-butylphenyl)-2-methyl-2-propenylidene]malononitrile, as matrix.⁵⁸ Infrared spectra were recorded on a 100 FTIR PerkinElmer spectrophotometer equipped with a universal attenuated total reflectance (UATR) accessory. Conductivities were measured in ca. 5×10^{-4} M acetone solutions of the complexes using a Philips PW 9501/01 conductivity meter.

The absolute molecular weight averages (M_n and M_w), polydispersity index (PDI, M_w/M_n), and molar mass distribution were determined by SEC-MALS at the Chromatography and Spectroscopy Service of the ISQCH. SEC-MALS analyses were carried out using a Waters 2695 instrument equipped with three PL-Gel Mixed B LS columns fitted to a MALS detector (miniDAWN Treos, Wyatt) and a differential refractive index detector (Optilab Rex, Wyatt). The polymer solutions in THF (≈ 2.0 mg/mL) were filtered through a $0.45 \mu\text{m}$ PTFE membrane filter before being injected into the GPC systems. To minimize sample degradation, the analyses were carried out immediately after the dissolution of the polymer sample in THF.^{59,60} Data analysis was performed with ASTRA Software from Wyatt. The samples were eluted at 25°C with THF at a flow rate of 1.0 mL/min. The reported dn/dc value of $0.2864 \text{ mL}\cdot\text{g}^{-1}$ determined at 633 nm for atactic PPA⁵⁹ was used, which resulted in calculated mass recoveries that were in reasonable agreement with the theoretical values.⁶¹

Synthesis of Amino-Functionalized Phosphine Ligands. *General Method.* A glass reaction tube fitted with a greaseless high-vacuum stopcock was charged with the corresponding allylamine (10 mmol) and diphenylphosphine (2 mmol). The mixture was placed between two white lamps of 400 W and stirred for 5 days at room temperature. The obtained viscous oil was dissolved in *n*-hexane (2 mL) and transferred to a Schlenk tube under argon. The volatiles were removed under vacuum to give the compounds as colorless oily products.

$\text{Ph}_2\text{P}(\text{CH}_2)_3\text{NHMe}$. $\text{H}_2\text{C}=\text{CHCH}_2\text{NHMe}$ (1 mL, $\rho = 0.741 \text{ g}\cdot\text{mL}^{-1}$, 96%, 10 mmol), HPPPh_2 (355 μL , $\rho = 1.07 \text{ g}\cdot\text{mL}^{-1}$, 98%, 2 mmol). Yield: 82%. Anal. Calcd. for $\text{C}_{16}\text{H}_{20}\text{NP}$: C, 74.69; H, 7.83; N, 5.44. Found: C, 74.45; H, 7.81; N, 5.44. MS (ESI+, CH_2Cl_2 , m/z , %): 258.4 ($[\text{M} + \text{H}]^+$, 100). ^1H NMR (298 K, CDCl_3): δ 7.46–7.31 (m, 10H, Ph), 2.63 (t, $J_{\text{H-H}} = 7.0$, 2H, CH_2N), 2.41 (s, 3H, CH_3), 2.10 (m, 2H, CH_2P), 1.64 (m, 2H, CH_2), 1.29 (br, 1H, NH). $^{31}\text{P}\{^1\text{H}\}$ NMR (298 K, CDCl_3): δ -15.6 (s). $^{13}\text{C}\{^1\text{H}\}$ NMR (298 K, CDCl_3): δ 139.5 (d, $J_{\text{C-P}} = 10.1$, C_i), 132.7 (d, $J_{\text{C-P}} = 18.4$, C_o), 128.5 (C_p), 128.4 (d, $J_{\text{C-P}} = 6.6$, C_m), 53.1 (d, $J_{\text{C-P}} = 13.5$, CH_2N), 36.4 (s, CH_3), 26.2 (d, $J_{\text{C-P}} = 16.3$, CH_2P), 25.7 (d, $J_{\text{C-P}} = 11.5$, CH_2).

$\text{Ph}_2\text{P}(\text{CH}_2)_3\text{NH}_2$. $\text{H}_2\text{C}=\text{CHCH}_2\text{NH}_2$ (0.77 mL, $\rho = 0.761 \text{ g}\cdot\text{mL}^{-1}$, 98%, 10 mmol), HPPPh_2 (355 μL , $\rho = 1.07 \text{ g}\cdot\text{mL}^{-1}$, 98%, 2 mmol). Yield: 77%. Anal. Calcd. for $\text{C}_{15}\text{H}_{18}\text{NP}$: C, 74.05; H, 7.46; N, 5.76. Found: C, 74.19; H, 7.43; N, 5.75. MS (ESI+, CHCl_3 , m/z , %): 244.1 ($[\text{M} + \text{H}]^+$, 100). ^1H NMR (298 K, CDCl_3): δ 7.46–7.33 (m, 10H, Ph), 2.78 (t, $J_{\text{H-H}} = 7.0$, 2H, CH_2N), 2.06 (m, 2H, CH_2P), 1.57 (m, 2H, CH_2), 1.25 (br, 2H, NH_2). $^{31}\text{P}\{^1\text{H}\}$ NMR (298 K, CDCl_3): δ -16.0 (s). $^{13}\text{C}\{^1\text{H}\}$ NMR (298 K, CDCl_3): δ 138.7 (d, $J_{\text{C-P}} = 13.0$, C_i), 132.7 (d, $J_{\text{C-P}} = 18.4$, C_o), 128.5 (C_p), 128.4 (d, $J_{\text{C-P}} = 6.6$, C_m), 43.4 (d, $J_{\text{C-P}} = 13.7$, CH_2N), 30.2 (d, $J_{\text{C-P}} = 15.5$, CH_2P), 25.3 (d, $J_{\text{C-P}} = 11.7$, CH_2).

Synthesis of $[\text{Rh}(\text{nbd})\{\text{Ph}_2\text{P}(\text{C}_6\text{H}_4)\text{NMe}\}]$ (2**).** A yellow solution of $[\text{Rh}(\mu\text{-OMe})(\text{nbd})_2]$ (100 mg, 0.221 mmol in benzene (5 mL) was slowly added to a solution of $\text{Ph}_2\text{P}(\text{C}_6\text{H}_4)\text{NHMe}$ (129 mg, 0.442 mmol) in benzene (2 mL) to give immediately an orange solution. The solution was stirred for 15 min and then concentrated under vacuum to ca. 1 mL. Addition of *n*-hexane (3 mL) while stirring gave an orange solid, which was filtered, washed with conc. *n*-hexane (3×2 mL), and dried under vacuum. Yield: 73%. Anal. Calcd. for $\text{C}_{26}\text{H}_{25}\text{NPRh}$: C, 64.34; H, 5.19; N, 2.89. Found: C, 64.40; H, 5.18; N, 2.88. MS (MALDI-ToF, CH_2Cl_2 , m/z , %): 486.0 ($[\text{M} + \text{H}]^+$, 100).

^1H NMR (298 K, C_6D_6): δ 7.58 (s, 4H, Ph), 7.28 (m, 1H, H_{Ar}), 7.00 (m, 7H, Ph and H_{Ar}), 6.67 (m, 1H, H_{Ar}), 6.45 (m, 1H, H_{Ar}), 4.85 (br, 2H, =CH nbd), 3.50 (br, 2H, CH nbd), 3.25 (br, 2H, =CH nbd), 2.89 (s, 3H, CH_3), 1.29 (m, 2H, CH_2 nbd). $^{31}\text{P}\{^1\text{H}\}$ NMR (298 K, C_6D_6): δ 38.4 (d, $J_{\text{P-Rh}} = 183.1$). $^{13}\text{C}\{^1\text{H}\}$ NMR (298 K, C_6D_6): δ 170.0 (dd, $J_{\text{C-P}} = 28.3$, $J_{\text{C-Rh}} = 3.5$, $\text{C}_{\text{i-N-Ar}}$), 133.8 (C_{Ar}), 133.8 (C_{Ar}), 133.0 (d, $J_{\text{C-P}} = 12.3$, C_{O} , Ph), 132.6 (dd, $J_{\text{C-P}} = 44.2$, $J_{\text{C-Rh}} = 1.9$, C_{P} , Ph), 129.9 (d, $J_{\text{C-P}} = 2.2$, C_{P} , Ph), 128.7 (d, $J_{\text{C-P}} = 10.0$, C_{m} , Ph), 117.2 (dd, $J_{\text{C-P}} = 48.3$, $J_{\text{C-Rh}} = 1.1$, $\text{C}_{\text{i-P-Ar}}$), 113.4 (d, $J_{\text{C-P}} = 7.1$, C_{Ar}), 109.9 (dd, $J_{\text{C-P}} = 14.0$, $J_{\text{C-Rh}} = 1.7$, C_{Ar}), 86.6 (d, $J_{\text{C-Rh}} = 6.0$, =CH nbd), 86.5 (d, $J_{\text{C-Rh}} = 5.7$, =CH nbd), 64.4 (dd, $J_{\text{C-Rh}} = 4.4$, $J_{\text{C-P}} = 1.9$, CH_2 nbd), 52.2 (CH nbd), 49.8 (d, $J_{\text{C-Rh}} = 9.8$, =CH nbd), 39.1 (CH_3).

Synthesis of $[\text{Rh}_2(\text{diene})\{\mu\text{-NH}(\text{CH}_2)_3\text{PPh}_2\}_2]$. *General Method.* In a dry box, potassium bis(trimethylsilyl)amide (KHDMS) was added to a solution of $\text{Ph}_2\text{P}(\text{CH}_2)_3\text{NH}_2$ in THF (2 mL). The solution was transferred to a suspension of the corresponding dinuclear compound $[\text{Rh}(\mu\text{-Cl})(\text{diene})]_2$ in THF (8 mL) to give red solutions, which were stirred for 1 h at room temperature. The solutions were filtered to eliminate the KCl formed and then brought to dryness under vacuum to give red-orange solids, which were washed with *n*-hexane (3×2 mL) and dried under vacuum. Recrystallization from THF/*n*-hexane was necessary to obtain pure compounds.

$[\text{Rh}_2(\text{cod})\{\mu\text{-NH}(\text{CH}_2)_3\text{PPh}_2\}_2]$ (3). $[\text{Rh}(\mu\text{-Cl})(\text{cod})]_2$ (100 mg, 0.203 mmol), $\text{Ph}_2\text{P}(\text{CH}_2)_3\text{NH}_2$ (98.8 mg, 0.406 mmol), KHDMS (82 mg, 0.411 mmol). Yield: 76%. Anal. Calcd. for $\text{C}_{38}\text{H}_{46}\text{N}_2\text{P}_2\text{Rh}_2$: C, 57.16; H, 5.81; N, 3.51. Found: C, 57.32; H, 5.82; N, 3.50. MS (ESI+, THF, m/z , %): 589.1 ($[\text{Rh}(\text{Ph}_2\text{P}(\text{CH}_2)_3\text{NH}_2)_2]^+$, 100), 454.2 ($[\text{Rh}(\text{cod})(\text{Ph}_2\text{P}(\text{CH}_2)_3\text{NH}_2)]^+$, 20). ^1H NMR (298 K, C_6D_6): δ 7.93 (m, 4H, Ph), 7.46 (m, 4H, Ph), 7.07–6.88 (m, 12H, Ph), 3.88 (br, 2H, =CH cod), 3.66 (br, 2H, =CH cod), 2.82 (m, 4H, $\text{CH}_2\text{N} + \text{CH}_2$), 2.60 (m, 2H, CH_2P), 2.27 (m, 2H, CH_2N), 2.09 (m, 4H, $\text{CH}_2\text{P} + \text{CH}_2$), 1.91 (m, 2H, CH_2 cod), 1.79 (m, 2H, CH_2 cod), 1.54 (m, 2H, CH_2 cod), 1.37 (m, 2H, CH_2 cod), –0.17 (m, 2H, NH). $^{31}\text{P}\{^1\text{H}\}$ NMR (298 K, C_6D_6): δ 38.0 (d, $J_{\text{P-Rh}} = 172.0$). $^{13}\text{C}\{^1\text{H}\}$ NMR (298 K, C_6D_6): δ 138.8 (d, $J_{\text{C-P}} = 8.3$, C_{i}), 138.4 (d, $J_{\text{C-P}} = 9.0$, C_{i}), 134.0 (m, C_{O}), 133.7 (m, C_{O}), 130.9 (m, C_{m}), 128.4 (m, C_{m}), 127.0 (C_{P}), 126.9 (C_{P}), 75.6 (d, $J_{\text{C-Rh}} = 12.4$, =CH cod), 75.4 (d, $J_{\text{C-Rh}} = 12.6$, =CH cod), 47.3 (CH_2N), 32.1 (CH_2P), 31.4 (CH_2), 29.6 (br, CH_2 cod), 29.5 (d, $J_{\text{C-Rh}} = 17.2$, CH_2 cod), 29.2 (d, $J_{\text{C-Rh}} = 11.8$, CH_2 cod).

$[\text{Rh}_2(\text{nbd})\{\mu\text{-NH}(\text{CH}_2)_3\text{PPh}_2\}_2]$ (4). $[\text{Rh}(\mu\text{-Cl})(\text{nbd})]_2$ (100 mg, 0.217 mmol), $\text{Ph}_2\text{P}(\text{CH}_2)_3\text{NH}_2$ (106 mg, 0.434 mmol), KHDMS (88 mg, 0.441 mmol). Yield: 68%. Anal. Calcd. for $\text{C}_{37}\text{H}_{42}\text{N}_2\text{P}_2\text{Rh}_2$: C, 56.79; H, 5.41; N, 3.58. Found: C, 56.77; H, 5.41; N, 3.57. MS (ESI+, THF, m/z , %): 589.1 ($[\text{Rh}(\text{Ph}_2\text{P}(\text{CH}_2)_3\text{NH}_2)_2]^+$, 30), 438 ($[\text{Rh}(\text{nbd})(\text{Ph}_2\text{P}(\text{CH}_2)_3\text{NH}_2)]^+$, 100). ^1H NMR (298 K, C_6D_6): δ 7.97 (m, 4H, Ph), 7.51 (m, 4H, Ph), 7.07–6.95 (m, 12H, Ph), 4.08 (br, 1H, CH nbd), 3.50 (br, 2H, CH nbd), 2.82 (m, 2H, CH_2N), 2.19 (m, 2H, CH_2N), 2.12 (m, 2H, CH_2P), 1.90 (m, 2H, CH_2), 1.78 (m, 2H, CH_2), 1.45 (br, 2H, =CH nbd), 1.42 (br, 2H, =CH nbd), 1.60 (m, 1H, CH_2 nbd), 1.28 (br, 1H, CH_2 nbd + 2H, NH), 0.01 (m, 2H, CH_2P). $^{31}\text{P}\{^1\text{H}\}$ NMR (298 K, C_6D_6): δ 36.8 (d, $J_{\text{P-Rh}} = 173.21$). $^{13}\text{C}\{^1\text{H}\}$ NMR (298 K, C_6D_6): δ 138.3 (dd, $J_{\text{C-P}} = 36.5$, $J_{\text{C-Rh}} = 5.6$, C_{i}), 133.8 (dt, $J_{\text{C-P}} = 17.1$, $J_{\text{C-Rh}} = 5.9$, C_{O}), 128.3 (C_{P}), 126.9 (dd, $J_{\text{C-P}} = 8.5$, $J_{\text{C-Rh}} = 4.0$, C_{m}), 60.5 (d, $J_{\text{C-Rh}} = 5.5$, CH_2 nbd), 52.6 (d, $J_{\text{C-Rh}} = 9.8$, =CH nbd), 52.3 (d, $J_{\text{C-Rh}} = 10.3$, =CH nbd), 51.1 (br, CH nbd), 49.1 (CH_2N), 29.5 (CH_2), 29.4 (d, $J_{\text{C-P}} = 23.7$, CH_2P).

$[\text{Rh}_2(\text{tfb})\{\mu\text{-NH}(\text{CH}_2)_3\text{PPh}_2\}_2]$ (5). $[\text{Rh}(\mu\text{-Cl})(\text{tfb})]_2$ (100 mg, 0.137 mmol), $\text{Ph}_2\text{P}(\text{CH}_2)_3\text{NH}_2$ (66.7 mg, 0.274 mmol), KHDMS (56 mg, 0.281 mmol). Yield: 70%. Anal. Calcd. for $\text{C}_{42}\text{H}_{46}\text{F}_4\text{N}_2\text{P}_2\text{Rh}_2$: C, 55.04; H, 4.40; N, 3.06. Found: C, 55.36; H, 4.18; N, 2.95. MS (ESI+, THF, m/z , %): 589.1 ($[\text{Rh}(\text{Ph}_2\text{P}(\text{CH}_2)_3\text{NH}_2)_2]^+$, 100). ^1H NMR (298 K, C_6D_6): δ 7.91 (m, 4H, Ph), 7.51 (m, 4H, Ph), 7.11–6.97 (m, 12H, Ph), 5.93 (br, 1H, CH tfb), 5.66 (br, 1H, CH tfb), 3.18 (m, 2H, =CH tfb), 3.14 (m, 2H, =CH tfb), 2.94 (m, 2H, CH_2N), 2.19 (m, 2H, CH_2), 2.01 (m, 2H, CH_2N), 1.57 (m, 2H, CH_2), 1.43 (m, 2H, CH_2P), 1.09 (br, 2H, NH), 0.28 (m, 2H, CH_2P). $^{31}\text{P}\{^1\text{H}\}$ NMR (298 K, C_6D_6): δ 37.0 (d, $J_{\text{P-Rh}} = 173.2$). ^{19}F NMR (298 K, CDCl_3): δ –148.73 (m, 2F, tfb), –149.58 (s, 4F, BF_4), –161.81 (m, 2F, tfb). $^{13}\text{C}\{^1\text{H}\}$ NMR (298 K, CDCl_3): δ 139.4 (d, $J_{\text{C-F}} = 230.9$, C-

F tfb), 138.4 (d, $J_{\text{C-P}} = 18.8$, C_{i}), 138.2 (d, $J_{\text{C-P}} = 19.5$, C_{i}), 138.6 (d, $J_{\text{C-P}} = 25.5$, C-F tfb), 134.1 (m, C_{O}), 128.5 (C_{P}), 127.41 (m, C_{m}), 51.2 (d, $J_{\text{C-Rh}} = 10.6$, =CH tfb), 50.9 (d, $J_{\text{C-Rh}} = 10.0$, =CH tfb), 50.1 (CH_2N), 40.8 (CH tfb), 40.6 (CH tfb), 29.6 (d, $J_{\text{C-P}} = 24.2$, CH_2P), 29.4 (CH_2).

Synthesis of $[\text{Rh}(\text{diene})(\text{Ph}_2\text{P}(\text{CH}_2)_3\text{NHR})][\text{BF}_4]$ (R = Me, H). *General Method.* AgBF_4 was added to a suspension of the corresponding dinuclear compound $[\text{Rh}(\mu\text{-Cl})(\text{diene})]_2$ in THF (10 mL) and the reaction mixture stirred for 30 min in the dark. The suspension was filtered and washed with THF (3×1 mL). The resulting solution was concentrated under vacuum to ca. 5 mL and then added slowly to a solution of the functionalized phosphine, $\text{Ph}_2\text{P}(\text{CH}_2)_3\text{NHMe}$ or $\text{Ph}_2\text{P}(\text{CH}_2)_3\text{NH}_2$, in THF (5 mL) at 273 K giving immediately yellow suspensions of the compounds. The solvent was removed under vacuum, and the yellow residue washed with diethyl ether (3×2 mL) and dried under vacuum.

$[\text{Rh}(\text{cod})(\text{Ph}_2\text{P}(\text{CH}_2)_3\text{NHMe})][\text{BF}_4]$ (6). $[\text{Rh}(\mu\text{-Cl})(\text{cod})]_2$ (100 mg, 0.203 mmol), AgBF_4 (79.0 mg, 0.406 mmol), $\text{Ph}_2\text{P}(\text{CH}_2)_3\text{NHMe}$ (104 mg, 0.406 mmol). Yield: 72%. Anal. Calcd. for $\text{C}_{24}\text{H}_{32}\text{BF}_4\text{NPRh}$: C, 51.92; H, 5.81; N, 2.52. Found: C, 51.64; H, 5.74; N, 2.48. MS (MALDI-Tof, CH_2Cl_2 , m/z , %): 468.1 ($[\text{M}]^+$, 100). Λ_{M} (acetone, 5.0×10^{-4} M) = $42 \Omega^{-1} \text{cm}^2 \text{mol}^{-1}$. ^1H NMR (298 K, CD_2Cl_2): δ 8.01 (m, 2H, Ph), 7.65 (m, 3H, Ph), 7.37 (m, 3H, Ph), 7.09 (m, 2H, Ph), 5.39 (br, 1H, =CH cod), 5.05 (br, 1H, =CH cod), 4.10 (br, 1H, NH), 3.73 (br, 1H, =CH cod), 3.16 (m, 1H, CH_2), 3.03–2.88 (m, 2H, 1H =CH cod, 1H, CH_2), 2.68–1.97 (m, 8H; 6H, CH_2 cod, 2H, CH_2), 2.23 (d, $J_{\text{H-H}} = 6.1$, 3H, CH_3), 2.12–1.86 (m, 3H; 1H, CH_2 , 2H, CH_2 cod), 1.68 (m, 1H, CH_2). $^{31}\text{P}\{^1\text{H}\}$ NMR (298 K, CD_2Cl_2): δ 17.0 (d, $J_{\text{P-Rh}} = 155.2$). $^{13}\text{C}\{^1\text{H}\}$ NMR (298 K, CD_2Cl_2): δ 135.6 (d, $J_{\text{C-P}} = 12.6$, C_{O}), 133.0 (d, $J_{\text{C-P}} = 2.2$, C_{P}), 131.5 (d, $J_{\text{C-P}} = 9.0$, C_{O}), 131.0 (d, $J_{\text{C-P}} = 9.3$, C_{i}), 130.9 (d, $J_{\text{C-P}} = 2.3$, C_{P}), 130.2 (d, $J_{\text{C-P}} = 10.2$, C_{m}), 129.9 (d, $J_{\text{C-P}} = 12.7$, C_{i}), 129.3 (d, $J_{\text{C-P}} = 9.6$, C_{m}), 108.5 (dd, $J_{\text{C-Rh}} = 9.7$, $J_{\text{C-P}} = 6.8$, =CH cod), 105.0 (dd, $J_{\text{C-Rh}} = 10.8$, $J_{\text{C-P}} = 6.8$, =CH cod), 79.1 (d, $J_{\text{C-Rh}} = 12.1$, =CH cod), 76.1 (d, $J_{\text{C-Rh}} = 11.6$, =CH cod), 53.3 (d, $J_{\text{C-P}} = 3.1$, CH_2N), 39.5 (CH_3), 33.8, 31.0, 30.7, 28.3 (CH_2 cod), 24.0 (d, $J_{\text{C-P}} = 25.2$, CH_2P), 19.2 (CH_2).

$[\text{Rh}(\text{nbd})(\text{Ph}_2\text{P}(\text{CH}_2)_3\text{NHMe})][\text{BF}_4]$ (7). $[\text{Rh}(\mu\text{-Cl})(\text{nbd})]_2$ (100 mg, 0.217 mmol), AgBF_4 (84.5 mg, 0.434 mmol), $\text{Ph}_2\text{P}(\text{CH}_2)_3\text{NHMe}$ (112 mg, 0.434 mmol). Yield: 58%. Anal. Calcd. for $\text{C}_{23}\text{H}_{28}\text{BF}_4\text{NPRh}$: C, 51.24; H, 5.24; N, 2.60. Found: C, 51.20; H, 5.21; N, 2.59. MS (MALDI-Tof, CH_2Cl_2 , m/z , %): 452.1 ($[\text{M}]^+$, 100). Λ_{M} (acetone, 5.0×10^{-4} M) = $46 \Omega^{-1} \text{cm}^2 \text{mol}^{-1}$. ^1H NMR (298 K, CD_2Cl_2): δ 7.77 (m, 2H, Ph), 7.57 (m, 3H, Ph), 7.44 (m, 3H, Ph), 7.24 (m, 2H, Ph), 5.65 (br, 1H, =CH nbd), 5.53 (br, 1H, =CH nbd), 3.95 (br, 1H, CH nbd), 3.87 (m, 2H, CH nbd y NH), 3.56 (br, 1H, =CH nbd), 3.24 (br, 1H, =CH nbd), 3.06 (t, $J_{\text{H-H}} = 11.9$, 1H, CH_2N), 2.82 (m, 1H, CH_2N), 2.44 (m, 1H, CH_2P), 2.35 (m, 1H, CH_2P), 2.29 (d, $J_{\text{H-H}} = 6.1$, 3H, CH_3), 1.82 (m, 1H, CH_2), 1.65 (m, 1H, CH_2), 1.48 (d, $J_{\text{H-H}} = 11.5$, 2H, CH_2 nbd). $^{31}\text{P}\{^1\text{H}\}$ NMR (298 K, CD_2Cl_2): δ 20.9 (d, $J_{\text{P-Rh}} = 171.8$). $^{13}\text{C}\{^1\text{H}\}$ NMR (298 K, CD_2Cl_2): δ 134.6 (d, $J_{\text{C-P}} = 12.4$, C_{O}), 132.3 (C_{P}), 132.2 (d, $J_{\text{C-P}} = 10.5$, C_{O}), 131.1 (C_{P}), 131.0 (d, $J_{\text{C-P}} = 9.6$, C_{i}), 130.5 (d, $J_{\text{C-P}} = 14.1$, C_{i}), 130.0 (d, $J_{\text{C-P}} = 10.2$, C_{m}), 129.6 (d, $J_{\text{C-Rh}} = 10.0$, C_{m}), 92.0 (br, =CH nbd), 90.8 (br, =CH nbd), 66.6 (dd, $J_{\text{C-Rh}} = 4.9$, $J_{\text{C-P}} = 1.6$, CH_2 nbd), 63.0 (d, $J_{\text{C-P}} = 12.0$, =CH nbd), 59.7 (d, $J_{\text{C-P}} = 9.5$, =CH nbd), 54.5 (d, $J_{\text{C-P}} = 4.9$, CH_2N), 53.3 (CH nbd), 53.1 (CH nbd), 38.7 (CH_3), 24.3 (d, $J_{\text{C-P}} = 24.8$, CH_2P), 20.7 (CH_2).

$[\text{Rh}(\text{tfb})(\text{Ph}_2\text{P}(\text{CH}_2)_3\text{NHMe})][\text{BF}_4]$ (8). $[\text{Rh}(\mu\text{-Cl})(\text{tfb})]_2$ (100 mg, 0.137 mmol), AgBF_4 (53.4 mg, 0.274 mmol), $\text{Ph}_2\text{P}(\text{CH}_2)_3\text{NHMe}$ (70.6 mg, 0.274 mmol). Yield: 62%. Anal. Calcd. for $\text{C}_{28}\text{H}_{26}\text{BF}_8\text{NPRh}$: C, 49.96; H, 3.89; N, 2.08. Found: C, 50.08; H, 3.85; N, 2.08. MS (MALDI-Tof, CH_2Cl_2 , m/z , %): 586.1 ($[\text{M}]^+$, 100). Λ_{M} (acetone, 5.0×10^{-4} M) = $44 \Omega^{-1} \text{cm}^2 \text{mol}^{-1}$. ^1H NMR (298 K, CD_2Cl_2): δ 7.90 (m, 2H, Ph), 7.70–7.62 (m, 3H, Ph), 7.51–7.42 (m, 3H, Ph), 7.27 (m, 2H, Ph), 5.71 (br, 3H, CH tfb and =CH tfb), 5.41 (br, 1H, =CH tfb), 4.32 (br, 1H, NH), 3.30 (s, 1H, =CH tfb), 3.13 (m, 1H, CH_2N), 2.87 (m, 2H, =CH tfb and CH_2N), 2.55–2.41 (m, 2H, CH_2P), 2.38 (d, $J_{\text{H-H}} = 6.0$, 3H, CH_3), 1.99 (m, 1H, CH_2), 1.79 (m, 1H, CH_2). ^{31}P NMR (298 K, CD_2Cl_2): δ 21.4 (d, $J_{\text{P-Rh}} = 172.0$). $^{13}\text{C}\{^1\text{H}\}$ NMR (298 K, CD_2Cl_2): δ 140.3 (d, $J_{\text{C-F}} =$

242.6, C-F tff), 138.7 (d, $J_{C-P} = 152.4$, C-F tff), 134.7 (d, $J_{C-P} = 12.5$, C_o), 132.7 (C_p), 131.9 (d, $J_{C-P} = 10.3$, C_o), 131.3 (C_p), 130.2 (d, $J_{C-P} = 10.4$, C_m), 129.7 (d, $J_{C-P} = 9.9$, C_m), 129.3 (br, C_i), 127.6 (d, $J_{C-P} = 16.3$, C_i), 92.5 (br, =CH tff), 91.7 (br, =CH tff), 62.1 (d, $J_{C-Rh} = 12.7$, =CH tff), 58.9 (d, $J_{C-Rh} = 9.3$, =CH tff), 54.3 (d, $J_{C-Rh} = 5.1$, CH_2N), 42.5 (br, CH tff), 39.1 (CH_3), 23.9 (d, $J_{C-P} = 25.6$, CH_2P), 20.6 (CH_2).

Synthesis of [Rh(nbd){Ph₂P(CH₂)₃NH₂}] [BF₄] (9). [Rh(μ -Cl)(nbd)]₂ (100 mg, 0.217 mmol), AgBF₄ (84.5 mg, 0.434 mmol), Ph₂P(CH₂)₃NH₂ (105 mg, 0.434 mmol). Yield: 65%. Anal. Calcd. for C₂₂H₂₆BF₄N₂P₂Rh: C, 50.32; H, 4.99; N, 2.67. Found: C, 50.19; H, 5.05; N, 2.47. MS (MALDI-ToF, CH₂Cl₂, m/z , %): 438.0 ([M]⁺, 100). Λ_M (acetone, 5.0 $\times 10^{-4}$ M) = 57 Ω^{-1} cm² mol⁻¹. ¹H NMR (243 K, CD₂Cl₂): δ 7.52 (m, 10H, Ph), 5.49 (br, 2H, =CH nbd), 3.89 (br, 2H, CH nbd), 3.37 (m, 2H, =CH nbd), 2.93 (m, 2H, CH₂N), 2.86 (br, 2H, NH₂), 2.33 (m, 2H, CH₂P), 1.68 (m, 2H, CH₂), 1.49 (m, 2H, CH₂ nbd). ³¹P{¹H} NMR (243 K, CD₂Cl₂): δ 20.1 (d, $J_{P-Rh} = 169.3$). ¹³C{¹H} NMR (243K, CD₂Cl₂): δ 133.0 (d, $J_{C-P} = 11.6$, C_o), 131.2 (C_p), 130.1 (d, $J_{C-P} = 44.6$, C_i), 129.2 (d, $J_{C-P} = 10.0$, C_m), 90.3 (dd, $J_{C-Rh} = 9.4$, $J_{C-P} = 5.4$, =CH nbd), 66.0 (d, $J_{C-Rh} = 7.5$, CH₂ nbd), 60.9 (d, $J_{C-Rh} = 10.8$, =CH nbd), 52.9 (m, CH nbd), 43.4 (d, $J_{C-P} = 6.3$, CH₂N), 23.9 (d, $J_{C-P} = 30.9$, CH₂P), 23.8 (CH_2).

Synthesis of [Rh(nbd){Ph₂P(C₆H₄)NHMe}] [BF₄] (10). HBF₄·Et₂O (20.3 μ L, $\rho = 1.19$ g·mL⁻¹, 0.150 mmol) was added to a solution of [Rh(nbd){Ph₂P(C₆H₄)NMe}] (2) (50 mg, 0.103 mmol) in CH₂Cl₂ (5 mL) at 273 K. The solution was stirred for 30 min to give a yellow solution, which was brought to dryness under vacuum. The oily residue was triturated with cold diethyl ether to give a yellow solid, which was filtered, washed with diethyl ether (3 \times 3 mL), and dried under vacuum. Yield: 60%. Anal. Calcd. for C₂₆H₂₆BF₄N₂P₂Rh: C, 54.48; H, 4.57; N, 2.44. Found: C, 54.48; H, 4.52; N, 2.44. MS (MALDI-ToF, CH₂Cl₂, m/z , %): 486.0 ([M]⁺, 100). Λ_M (acetone, 5.0 $\times 10^{-4}$ M) = 45 Ω^{-1} cm² mol⁻¹. ¹H NMR (298K, CD₂Cl₂): δ 7.66–7.32 (m, 14H, Ph y H_{Ar}), 6.15 (d, $J_{H-H} = 5.9$, 1H, NH), 6.03 (br, 1H, =CH nbd), 5.56 (br, 1H, =CH nbd), 4.27 (br, 1H, =CH nbd), 4.11 (br, 1H, CH nbd), 4.02 (br, 1H, CH nbd), 3.95 (br, 1H, =CH nbd), 2.74 (d, $J_{H-H} = 5.9$, 3H, CH₃), 1.62 (m, 2H, CH₂ nbd). ³¹P{¹H} NMR (298 K, CD₂Cl₂): δ 37.0 (d, $J_{Rh-P} = 174.2$). ¹³C{¹H} NMR (298 K, CD₂Cl₂): δ 156.2 (d, $J_{C-P} = 21.0$, C_{i-N-Ar}), 134.3 (d, $J_{C-P} = 2.0$, C_{Ar}), 133.6 (d, $J_{C-P} = 12.5$, C_o Ph), 133.6 (C_{Ar}), 132.9 (d, $J_{C-P} = 12.1$, C_o Ph), 132.0 (C_p Ph), 131.5 (C_p Ph), 130.7 (d, $J_{C-P} = 42.7$, C_{i-P-Ar}), 130.4 (d, $J_{C-P} = 10.3$, C_i), 131.0 (d, $J_{C-P} = 10.4$, C_m Ph), 129.6 (d, $J_{C-P} = 10.9$, C_m Ph), 129.1 (d, $J = 5.8$, C_{Ar}), 128.5 (d, $J_{C-P} = 45.3$, C_i), 126.0 (d, $J_{C-P} = 10.0$, C_{Ar}), 93.9 (m, =CH nbd), 92.0 (m, =CH nbd), 67.4 (d, $J_{C-Rh} = 3.5$, CH₂ nbd), 66.4 (d, $J_{C-Rh} = 10.2$, =CH nbd), 60.4 (d, $J_{C-Rh} = 10.3$, =CH nbd), 54.3, 54.1 (CH nbd), 43.9 (CH_3).

Synthesis of [Rh{Ph₂P(CH₂)₃Z}] [BF₄] (Z = NHMe (11), NH₂ (12)). *General Method.* In a dry box, AgBF₄ was added to a suspension of [Rh(μ -Cl)(coe)₂]₂ in THF (10 mL) and the reaction mixture stirred for 30 min in the dark. The suspension was filtered and washed with THF (3 \times 1 mL). The resulting yellow solution was concentrated under vacuum to ca. 5 mL and added slowly to a solution of the corresponding amino-phosphine, Ph₂P(CH₂)₃NHMe or Ph₂P(CH₂)₃NH₂, in THF (2 mL) to give immediately an orange-red solution. The solution was stirred for 30 min and the solvent removed under vacuum to give an orange residue, which was washed with diethyl ether (3 \times 2 mL) and dried under vacuum.

[Rh{Ph₂P(CH₂)₃NHMe}] [BF₄] (11). [Rh(μ -Cl)(coe)₂]₂ (100 mg, 0.139 mmol), AgBF₄ (54.3 mg, 0.278 mmol), Ph₂P(CH₂)₃NHMe (71.7 mg, 0.279 mmol) in THF. Yield: 55%. Anal. Calcd. for C₃₂H₄₀BF₄N₂P₂Rh: C, 54.57; H, 5.72; N, 3.98. Found: C, 54.27; H, 5.92; N, 4.01. MS (MALDI-ToF, THF, m/z , %): 617.2 ([M]⁺, 100). ¹H NMR (298K, THF-*d*₈): δ 8.24 (m, 2H, Ph), 7.81 (m, 2H, Ph), 7.50 (m, 10H, Ph), 6.88 (m, 2H, Ph), 6.67 (m, 2H, Ph), 6.61 (m, 2H, Ph), 3.82 (br, 2H, NH), 3.25 (m, 2H, CH₂N), 2.78 (m, 2H, CH₂N), 2.43 (d, $J_{H-H} = 6.0$, 6H, CH₃), 2.25 (m, 4H, CH₂P), 1.79 (m, 2H, CH₂), 1.47 (m, 2H, CH₂). ³¹P{¹H} NMR (298K, THF-*d*₈): δ 36.2 (d, $J_{P-Rh} = 174.3$). ¹³C{¹H} NMR (298K, THF-*d*₈): δ 138.4 (d, $J_{C-P} =$

25.7, C_i), 138.1 (d, $J_{C-P} = 26.3$, C_i), 136.3 (dd, $J_{C-Rh} \approx J_{C-P} = 6.2$, C_o), 130.7 (dd, $J_{C-P} = 30.7$, $J_{C-Rh} = 9.8$, C_o), 130.6 (d, $J_{C-P} = 9.1$, C_m), 128.7 (d, $J_{C-P} = 11.7$, C_m), 128.9 (t, $J_{C-P} \approx J_{C-Rh} = 4.7$, C_m), 127.7 (t, $J_{C-P} \approx J_{C-Rh} = 4.8$, C_p), 127.1 (ft, $J_{C-P} \approx J_{C-Rh} = 4.5$, C_p), 54.6 (CH_2N), 40.3 (CH_3), 30.8 (CH_2P), 20.95 (CH_2).

[Rh{Ph₂P(CH₂)₃NH₂}] [BF₄] (12). [Rh(μ -Cl)(coe)₂]₂ (100 mg, 0.139 mmol), AgBF₄ (54.3 mg, 0.278 mmol), Ph₂P(CH₂)₃NH₂ (67.8 mg, 0.279 mmol) in THF. Yield: 62%. Anal. Calcd. for C₃₀H₃₆BF₄N₂P₂Rh: C, 53.28; H, 5.37; N, 4.14. Found: C, 53.72; H, 5.44; N, 4.07. MS (MALDI-ToF, THF, m/z , %): 589.1 ([M]⁺, 100). ¹H NMR (298 K, C₆D₆): δ 7.96 (br, 2H, Ph), 7.81 (br, 2H, Ph), 7.44 (m, 8H, Ph), 7.10 (m, 4H, Ph), 6.93 (m, 4H, Ph), 3.57 (br, 4H, NH₂), 2.94 (br, 4H, CH₂N), 1.88 (br, 4H, CH₂P), 1.06 (br, 4H, CH₂). ³¹P{¹H} NMR (298 K, C₆D₆): δ 39.0 (d, $J_{P-Rh} = 172.5$). ¹³C{¹H} NMR (298K, C₆D₆): 135.4 (m, C_i), 133.7 (br, C_o), 131.4 (br, C_p), 128.8 (br, C_m), 43.4 (br, CH₂N) 29.5 (m, CH₂P), 24.0 (CH_2).

Polymerization Reactions. The polymerization reactions were carried out in round-bottom flasks with efficient stirring. A typical polymerization procedure is as follows: phenylacetylene (70 μ L, 0.64 mmol) was added to a THF solution (2.5 mL) of the catalysts (6.4 μ mol) and the mixture stirred at 293 K in the absence of light. The consumption of monomer was monitored by GC using *n*-octane as internal standard. The polymer solutions were transferred into vigorously stirred cold methanol (25 mL, 273 K) using a cannula under argon. The polymers were filtered and washed with methanol and dried under vacuum to constant weight. The polymers were obtained as yellow-orange solids in good yields.

Crystal Structure Determinations. Suitable crystals for X-ray diffraction were obtained by slow evaporation of a solution of the compounds in benzene (2), *n*-hexane (4), or THF (11) and by slow diffusion of diethyl ether into a solution of the compound in tetrahydrofuran (7).

X-ray diffraction data were collected on a Bruker DUO (2, 4, and 7 complexes) or a Bruker Smart APEX (compound 11) diffractometers with graphite-monochromated Mo K α radiation ($\lambda = 0.71073$ Å) using narrow ω rotations (0.3°) at 100(2) K. Data reduction was performed with APEX 2 package; intensities were integrated with SAINT⁶² and corrected for absorption effects with SADABS program.⁶³ Structures were solved with direct methods with SHELXS^{64,65} and refined by full-matrix least-squares refinement on F^2 with SHELXL-2014,⁶⁶ included in WingX package.⁶⁷ Hydrogen atoms of N–H fragments in 4, 7, and 11 complexes have been included in the model in observed positions and freely refined. Particular refinement details are listed below.

Crystal Data and Structure Refinement for 2. C₂₆H₂₅N₂P₂Rh; $M = 485.35$; red plate, 0.053 \times 0.100 \times 0.219 mm³; orthorhombic, $P2_12_12_1$; $a = 8.9345(10)$ Å, $b = 11.5260(13)$ Å, $c = 20.337(2)$ Å; $Z = 4$; $V = 2094.3(4)$ Å³; $D_c = 1.539$ g·cm⁻³; $\mu = 0.904$ mm⁻¹; min. and max. absorption correction factors 0.795 and 0.920; $2\theta_{max} = 59.072^\circ$; 22882 collected reflections, 5503 unique reflections; $R_{int} = 0.0339$; number of data/restraint/parameters 5503/8/362; final GoF 1.054; $R_1 = 0.0245$ [5186 reflections, $I > 2\sigma(I)$]; $wR2 = 0.0548$ all data; Flack parameter: $-0.028(11)$; largest difference peak, 0.971 e·Å⁻³. Hydrogen atoms have been included in the model in observed positions and refined with some constraints concerning C–H bond lengths.

Crystal Data and Structure Refinement for 4. C₃₇H₄₂N₂P₂Rh₂; $M = 782.48$; yellow block, 0.080 \times 0.080 \times 0.168 mm³; triclinic; $a = 9.7240(9)$ Å, $b = 14.8703(13)$ Å, $c = 23.400(2)$ Å; $\alpha = 90.3980(10)$, $\beta = 98.1640(10)$, $\gamma = 91.7970(10)^\circ$; $Z = 4$; $V = 3347.4(5)$ Å³; $D_c = 1.553$ g·cm⁻³; $\mu = 1.110$ mm⁻¹; min. and max. absorption correction factors, 0.744 and 0.913; $2\theta_{max} = 59.142^\circ$; 481 310 collected reflections, 16 923 unique reflections; $R_{int} = 0.0350$; number of data/restraint/parameters 16 923/2/1100; final GoF 1.044; $R_1 = 0.0411$ [12 462 reflections, $I > 2\sigma(I)$]; $wR2 = 0.0915$ all data; largest difference peak, 0.997 e·Å⁻³. Hydrogen atoms have been included in the model in observed positions and refined with some constraints concerning C–H bond lengths.

Crystal Data and Structure Refinement for 7. $C_{23}H_{28}BF_4NPRh$; $M = 539.15$; brown needle, $0.052 \times 0.072 \times 0.293$ mm³; monoclinic, $P2_1/n$; $a = 14.1153(17)$ Å, $b = 10.6325(13)$ Å, $c = 16.002(2)$ Å; $\beta = 108.131(2)^\circ$; $Z = 4$; $V = 2282.4(5)$ Å³; $D_c = 1.569$ g·cm⁻³; $\mu = 0.861$ mm⁻¹; min. and max. absorption correction factors, 0.714 and 0.915; $2\theta_{max} = 52.574^\circ$; 16 648 collected reflections, 4608 unique reflections; $R_{int} = 0.0758$; number of data/restraint/parameters, 4608/0/305; final GoF, 1.020; $R_1 = 0.0504$ [4608 reflections, $I > 2\sigma(I)$]; $wR2 = 0.1066$ all data; largest difference peak, 1.131 e·Å⁻³. Carbon atoms of phenyl groups and two fluorine atoms of the counterion have been found to be disordered. They have been included in the model in two sets of positions and isotropically refined with complementary occupancy factors.

Crystal Data and Structure Refinement for 11. $C_{32}H_{40}BF_4N_2P_2Rh$; $M = 704.32$; yellow prism, $0.142 \times 0.208 \times 0.307$ mm³; monoclinic, $P2_1/n$; $a = 11.7793(6)$ Å, $b = 15.4800(8)$ Å, $c = 17.6167(9)$ Å; $\beta = 100.9310(10)^\circ$; $Z = 4$; $V = 3154.0(3)$ Å³; $D_c = 1.483$ g·cm⁻³; $\mu = 0.692$ mm⁻¹; min. and max. absorption correction factors, 0.800 and 0.894; $2\theta_{max} = 57.276^\circ$; 26 590 collected reflections, 7453 unique reflections; $R_{int} = 0.0326$; number of data/restraint/parameters, 7453/0/389; final GoF, 1.084; $R_1 = 0.0329$ [6426 reflections, $I > 2\sigma(I)$]; $wR2 = 0.0659$ all data; largest difference peak, 0.523 e·Å⁻³. Hydrogen atoms of amine groups have been included in the model in observed positions and freely refined.

■ ASSOCIATED CONTENT

Supporting Information

The Supporting Information is available free of charge on the ACS Publications website at DOI: 10.1021/acs.organomet.9b00078.

NMR spectra for selected compounds and selected chromatograms and conformational plots for PPA samples (PDF)

Accession Codes

CCDC 1894549–1894552 contain the supplementary crystallographic data for this paper. These data can be obtained free of charge via www.ccdc.cam.ac.uk/data_request/cif, or by emailing data_request@ccdc.cam.ac.uk, or by contacting The Cambridge Crystallographic Data Centre, 12 Union Road, Cambridge CB2 1EZ, UK; fax: +44 1223 336033.

■ AUTHOR INFORMATION

Corresponding Authors

*E-mail: vjimenez@unizar.es (M.V.J.).

*E-mail: perez@unizar.es (J.J.P.T.).

ORCID

M. Victoria Jiménez: 0000-0002-0545-9107

Luis A. Oro: 0000-0001-7154-7239

Jesús J. Pérez-Torrente: 0000-0002-3327-0918

Notes

The authors declare no competing financial interest.

■ ACKNOWLEDGMENTS

This article is dedicated to Prof. Pablo Espinet on the occasion of his 70th birthday. Financial support from the Spanish Ministry of Economy and Competitiveness (MINECO/FEDER) under the Projects CTQ2013-42532-P and CTQ2016-75884-P and the Diputación General de Aragón (DGA/E42_17R) is gratefully acknowledged.

■ REFERENCES

(1) Masuda, T. Substituted Polyacetylenes: Synthesis, Properties, and Functions. *Polym. Rev.* **2017**, *57*, 1–14.

(2) Xu, A.; Masuda, T.; Zhang, A. Stimuli-Responsive Polyacetylenes and Dendronized Poly(phenylacetylene)s. *Polym. Rev.* **2017**, *57*, 138–158.

(3) Masuda, T.; Sanda, F.; Shiotsuki, M. Polymerization of Acetylenes In *Comprehensive Organometallic Chemistry III*, 1st ed.; Michael, D., Mingos, P., Crabtree, R. H., Eds.; Elsevier: Amsterdam, Holanda, 2007; Vol. 11, pp 557–593.

(4) Shiotsuki, M.; Sanda, F.; Masuda, T. Polymerization of Substituted Acetylenes and Features of the Formed Polymers. *Polym. Chem.* **2011**, *2*, 1044–1058.

(5) Nikishkin, N. I.; Huskens, J.; Verboom, W. Highly active and robust rhodium(I) catalyst for the polymerization of arylacetylenes in polar and aqueous medium under air atmosphere. *Polymer* **2013**, *54*, 3175–3181.

(6) Casado, M. A.; Fazal, A.; Oro, L. A. Rhodium-Catalyzed Polymerization of Phenylacetylene and its Derivatives. *Arabian J. Sci. Eng.* **2013**, *38*, 1631–1646.

(7) Sedláček, J.; Vohlídal, J. Controlled and Living Polymerizations Induced with Rhodium Catalysts. A Review. *Collect. Czech. Chem. Commun.* **2003**, *68*, 1745–1790.

(8) Sedláček, J.; Balcar, H. Substituted Polyacetylenes Prepared with Rh Catalysts: From Linear to Network-Type Conjugated Polymers. *Polym. Rev.* **2017**, *57*, 31–54.

(9) Jiménez, M. V.; Pérez-Torrente, J. J.; Bartolomé, M. I.; Vispe, E.; Lahoz, F. J.; Oro, L. A. Cationic Rhodium Complexes with Hemilabile Phosphine Ligands as Polymerization Catalyst for High Molecular Weight Stereoregular Poly(phenylacetylene). *Macromolecules* **2009**, *42*, 8146–8156.

(10) Angoy, M.; Bartolomé, M. I.; Vispe, E.; Lebeda, P.; Jiménez, M. V.; Pérez-Torrente, J. J.; Collins, S.; Podzimek, S. Branched Poly(phenylacetylene). *Macromolecules* **2010**, *43*, 6278–6283.

(11) Angoy, M.; Jiménez, M. V.; Modrego, F. J.; Oro, L. A.; Passarelli, V.; Pérez-Torrente, J. J. Mechanistic Investigation on the Polymerization of Phenylacetylene by 2-Diphenylphosphinopyridine Rhodium(I) Catalysts: Understanding the Role of the Cocatalyst and Alkynyl Intermediates. *Organometallics* **2018**, *37*, 2778–2794.

(12) Trhlíková, O.; Zedník, J.; Balcar, H.; Brus, J.; Sedláčka, J. [Rh(cycloolefin)(acac)] Complexes as Catalysts of Polymerization of Aryl- and Alkylacetylenes: Influence of Cycloolefin Ligand and Reaction Conditions. *J. Mol. Catal. A: Chem.* **2013**, *378*, 57–66.

(13) Mastorilli, P.; Nobile, C. F.; Rizzuti, A.; Suranna, G. P.; Acierio, D.; Amendola, E. Polymerization of phenylacetylene and of p-tolylacetylene catalyzed by β -dioxigenato rhodium(I) complexes in homogeneous and heterogeneous phase. *J. Mol. Catal. A: Chem.* **2002**, *178*, 35–42.

(14) Wang, Q.; Jia, H.; Shi, Y.; Ma, L.; Yang, G.; Wang, Y.; Xu, S.; Wang, J.; Zang, Y.; Aoki, T. [Rh(L-alanine)(1,5-Cyclooctadiene)] Catalyzed Helix-Sense-Selective Polymerizations of Achiral Phenylacetylenes. *Polymers* **2018**, *10*, 1223.

(15) Jaseer, E. A.; Casado, M. A.; Al-Saadi, A. A.; Oro, L. A. Intermolecular Hydroamination versus Stereoregular Polymerization of Phenylacetylene by Rhodium Catalysts Based on N–O Bidentate Ligands. *Inorg. Chem. Commun.* **2014**, *40*, 78–81.

(16) Yim, J. C. H.; Schafer, L. Efficient Anti-Markovnikov-Selective Catalysts for Intermolecular Alkyne Hydroamination: Recent Advances and Synthetic Applications. *Eur. J. Inorg. Chem.* **2014**, 6825–6840.

(17) Müller, T. E.; Hultsch, K. C.; Yus, M.; Foubelo, F.; Tada, M. Hydroamination: Direct Addition of Amines to Alkenes and Alkynes. *Chem. Rev.* **2008**, *108*, 3795–3892.

(18) Desnoyer, A. N.; Love, J. A. Recent Advances in Well-Defined, Late Transition Metal Complexes that Make and/or Break C–N, C–O and C–S Bonds. *Chem. Soc. Rev.* **2017**, *46*, 197–238.

(19) Fryzuk, M. D.; McNeil, P. A. Stereoselective formation of iridium(III) amides and ligand-assisted heterolytic splitting of dihydrogen. *Organometallics* **1983**, *2*, 682–684.

(20) Schneider, S.; Meiners, J.; Askevold, B. Cooperative Aliphatic PNP Amido Pincer Ligands-Versatile Building Blocks for Coordination Chemistry and Catalysis. *Eur. J. Inorg. Chem.* **2012**, 412–429.

- (21) Xue, P.; Sung, H. S. Y.; Williams, I. D.; Jia, G. Alkyne Oligomerization Mediated by Rhodium Complexes with a Phosphino-sulfonamido Ligand and Isolation and Characterization of a Rhodacyclopentadiene Complex. *J. Organomet. Chem.* **2006**, *691*, 1945–1953.
- (22) Jiménez, M. V.; Pérez-Torrente, J. J.; Bartolomé, M. I.; Oro, L. A. Convenient Methods for the Synthesis of a Library of Hemilabile Phosphines. *Synthesis* **2009**, 1916–1922.
- (23) Hounjet, L. J.; McDonal, R.; Ferguson, M. J.; Cowie, M. Comparison of Structure and Reactivity of Phosphine-Amido and Hemilabile Phosphine-Amine Chelates of Rhodium. *Inorg. Chem.* **2011**, *50*, 5361–5378.
- (24) Groom, C. R.; Brun, I. J.; Lightfoot, M. P.; Ward, S. C. The Cambridge Structural Database. *Acta Crystallogr., Sect. B: Struct. Sci., Cryst. Eng. Mater.* **2016**, *72*, 171–179.
- (25) Hounjet, L. J.; Bierenstiel, M.; Ferguson, M. J.; McDonal, R.; Cowie, M. Mono- and Binuclear Complexes of Rhodium Involving a New Series of Hemilabile O-Phosphinoaniline Ligands. *Dalton Trans.* **2009**, 4213–4226.
- (26) Oro, L. A.; Fernández, M. J.; Modrego, F. J.; Foces-Foces, C.; Cano, F. H. Di-(μ -amido)dirhodium Complexes: Structure of $[\text{Rh}_2(\mu\text{-}(\text{NH})_2\text{naphth})\text{I}_2(\text{CO})_2(\text{PPh}_3)_2]$. *Angew. Chem., Int. Ed.* **1984**, *23*, 913–914.
- (27) Cooper, M. K.; Organ, G. J.; Duckworth, P. A.; Henrick, K.; McPartlin, M. Synthesis and Oxidation Reactions of Mono- and Dinuclear Rhodium Carbonyl Complexes of (*o*-Diphenylphosphinophenyl)amine, H_2L ; X-ray Structure Analysis of a Rhodium(II) Amido-bridged Dimer, $[\{\text{Rh}(\mu\text{-HL})(\text{CO})\text{Cl}\}_2]$. *EtOH. J. Chem. Soc. Dalton Trans.* **1988**, 2287–2292.
- (28) Takemoto, S.; Otsuki, S.; Hashimoto, Y.; Kamikawa, k.; Matsezaka, H. Divalent Dirhodium Imido Complexes: Formation, Structure, and Alkyne Cycloaddition Reactivity. *J. Am. Chem. Soc.* **2008**, *130*, 8904–8905.
- (29) Ishiwata, K.; Kuwata, S.; Ikariya, T. Hydrogen- and Oxygen-Driven Interconversion between Imido-Bridged Dirhodium(III) and Amido-Bridged Dirhodium(II) Complexes. *J. Am. Chem. Soc.* **2009**, *131*, 5001–5009.
- (30) Fernández, M. J.; Modrego, F. J.; Oro, L. A.; Apreada, M. C.; Cano, F. H.; Foces-Foces, C. Amides of Rhodium and Iridium Derived from 2-Aminothiophenol and Diaminonaphthalene: X-Ray Crystal Structure of $\text{Rh}_2(\mu\text{-}1,8\text{-}(\text{NH})_2\text{C}_{10}\text{H}_6)(\text{CO})_4$. *Inorg. Chim. Acta* **1989**, *157*, 61–64.
- (31) Mena, I.; Casado, M. A.; García-Orduña, P.; Polo, V.; Lahoz, F. J.; Fazal, A.; Oro, L. A. Direct Access to Parent Amido Complexes of Rhodium and Iridium through N-H Activation of Ammonia. *Angew. Chem., Int. Ed.* **2011**, *50*, 11735–11738.
- (32) Tejel, C.; Ciriano, M. A.; Bordonaba, M.; López, J. A.; Lahoz, F. J.; Oro, L. A. Structural and Dynamic Studies on Amido-Bridged Rhodium and Iridium Complexes. *Chem. - Eur. J.* **2002**, *8*, 3128–3138.
- (33) Palacios, L.; DiGiuseppe, A.; Opalinska, A.; Castarlenas, R.; Pérez-Torrente, J. J.; Lahoz, F. J.; Oro, L. A. Labile Rhodium(I)-N-Heterocyclic Carbene Complexes. *Organometallics* **2013**, *32*, 2768–2774.
- (34) Jiménez, M. V.; Bartolomé, M. I.; Pérez-Torrente, J. J.; Lahoz, F. J.; Oro, L. A. Rhodium(I) Complexes with Hemilabile Phosphines: Rational Design for Efficient Oxidative Amination Catalysts. *ChemCatChem* **2012**, *4*, 1298–1310.
- (35) Jiménez, M. V.; Pérez-Torrente, J. J.; Bartolomé, M. I.; Lahoz, F. J.; Oro, L. A. Rational Design of Efficient Rhodium Catalysts for the Anti-markovnikov Oxidative Amination of Styrene. *Chem. Commun.* **2010**, 46, 5322–5324.
- (36) Berstein, J.; Davis, R. E.; Shimoni, L.; Chang, N.-L. Patterns in Hydrogen Bonding: Functionality and Graph Set Analysis in Crystals. *Angew. Chem., Int. Ed.* **1995**, *34*, 1555–1573.
- (37) Furlani, A.; Napoletano, C.; Russo, M. V.; Camus, A.; Marsich, N. J. The Influence of the Ligands on the Catalytic Activity of a Series of Rh^{I} Complexes in Reactions with Phenylacetylene: Synthesis of Stereoregular Poly(phenyl)acetylene. *J. Polym. Sci., Part A: Polym. Chem.* **1989**, *27*, 75–86.
- (38) Furlani, A.; Napoletano, C.; Russo, M. V.; Feast, W. J. Stereoregular Polyphenylacetylene. *Polym. Bull.* **1986**, *16*, 311–317.
- (39) Saeed, I.; Shiotsuki, M.; Masuda, T. Effect of Diene Ligands in the Rhodium-catalyzed Polymerization of Phenylacetylene. *Macromolecules* **2006**, *39*, 8977–8981.
- (40) Onishi, N.; Shiotsuki, M.; Sanda, F.; Masuda, T. Polymerization of Phenylacetylenes with Rhodium Zwitterionic Complexes: Enhanced Catalytic Activity by π -acidic Diene Ligands. *Macromolecules* **2009**, *42*, 4071–4076.
- (41) Kishimoto, Y.; Miyatake, T.; Ikariya, T.; Noyori, R. An Efficient Rhodium(I) Initiator for Stereospecific Living Polymerization of Phenylacetylenes. *Macromolecules* **1996**, *29*, 5054–5055.
- (42) Kishimoto, Y.; Eckerle, P.; Miyatake, T.; Kainosho, M.; Ono, A.; Ikariya, T.; Noyori, R. Well-Controlled Polymerization of Phenylacetylenes with Organorhodium(I) Complexes: Mechanism and Structure of the Polyenes. *J. Am. Chem. Soc.* **1999**, *121*, 12035–12044.
- (43) Shiotsuki, M.; Onishi, N.; Sanda, F.; Masuda, T. Living Polymerization of Phenylacetylenes Catalyzed by Cationic Rhodium Complexes Bearing Tetrafluorobenzobarrelene. *Polym. J.* **2011**, *43*, 51–57.
- (44) Komatsu, H.; Suzuki, Y.; Yamazaki, H. Unprecedented Rhodium-Mediated Tetramerization of Bulky Terminal Alkynes Leading to Hydropentalenylrhodium Complexes. *Chem. Lett.* **2001**, *30*, 998–999.
- (45) Hall, H. K., Jr. Correlation of the Base Strengths of Amines. *J. Am. Chem. Soc.* **1957**, *79*, 5441–5444.
- (46) Cametti, C.; Codastefano, P.; D'Amato, R.; Furlani, A.; Russo, M. Static and Dynamic Light Scattering Measurements of Polyphenylacetylene (PPA) in Different Organic Solvents (Tetrahydrofuran, Toluene and Chloroform). *Synth. Met.* **2000**, *114*, 173–179.
- (47) Ara, I.; Berenguer, J. R.; Eguizábal, E.; Forniés, J.; Lalinde, E.; Martín, A.; Martínez, F. Synthesis, Characterization, and Reactivity of New Alkynyl Complexes of Rhodium and Iridium: Preparation of Neutral ($\text{M}-\text{M}'$: $\text{M} = \text{Rh}, \text{Ir}$; $\text{M}' = \text{Pt}, \text{Pd}$) Hetero-Alkynyl-Bridged Dinuclear Complexes. *Organometallics* **1998**, *17*, 4578–4596.
- (48) Schäfer, M.; Wolf, J.; Werner, H. Binding Two C_2 Units to an Electron-Rich Transition-Metal Center: The Interplay of Alkyne-(alkynyl), Bisalkynyl(hydrido), Alkynyl(vinylidene), Alkynyl(allene), Alkynyl(olefin), and Alkynyl(enyne) Rhodium Complexes. *Organometallics* **2004**, *23*, 5713–5728.
- (49) Zhu, X.; Ward, R. M.; Albesa-Jové, D.; Howard, J. A. K.; Porrés, L.; Beeby, A.; Low, P. J.; Wong, W.-K.; Marder, T. B. Synthesis of new mer,trans-Rhodium(III) Hydrido-bis(acetylide) Complexes: Structure of mer,trans- $[(\text{PMe}_3)_3\text{Rh}(\text{C}\equiv\text{C}-\text{C}_6\text{H}_4-4\text{-NMe}_2)_2\text{H}]$. *Inorg. Chim. Acta* **2006**, *359*, 2859–2863.
- (50) Zhang, P.; Wang, H.; Shi, X.; Yan, X.; Wu, X.; Zhang, S.; Yao, B.; Feng, X.; Zhi, J.; Li, X.; Tong, B.; Shi, J.; Wang, L.; Dong, Y. On-Water Polymerization of Phenylacetylene Catalyzed by Rh Complexes Bearing Strong π -Acidic Dibenzo[a,e]cyclooctatetraene Ligand. *J. Polym. Sci., Part A: Polym. Chem.* **2017**, *55*, 716–725.
- (51) Ke, Z.; Abe, S.; Ueno, T.; Morokuma, K. Rh-catalyzed Polymerization of Phenylacetylene: Theoretical Studies of the Reaction Mechanism, Regioselectivity, and Stereoregularity. *J. Am. Chem. Soc.* **2011**, *133*, 7926–7941.
- (52) Kishimoto, Y.; Itou, M.; Miyatake, T.; Ikariya, T.; Noyori, R. Polymerization of Monosubstituted Acetylenes with a Zwitterionic Rhodium(I) Complex, $\text{Rh}^+(2,5\text{-norbornadiene})[(\eta^6\text{-C}_6\text{H}_5\text{-B}^-(\text{C}_6\text{H}_5)_3)]$. *Macromolecules* **1995**, *28*, 6662–6666.
- (53) Onishi, N.; Shiotsuki, M.; Masuda, T.; Sano, N.; Sanda, F. Polymerization of Phenylacetylenes Using Rhodium Catalysts Coordinated by Norbornadiene Linked to a Phosphino or Amino Group. *Organometallics* **2013**, *32*, 846–853.
- (54) Giordano, G.; Crabtree, R. H.; Heintz, R. M.; Forster, D.; Morris, D. E. Di- μ -Chloro-Bis(η^4 -1,5-Cyclooctadiene) Dirhodium(I). In *Inorganic Syntheses*; John Wiley & Sons, Inc, 1979; Vol. 19, pp 218–220.

(55) Abel, E. W.; Benett, M. A.; Wilkinson, G. Norbornadiene–metal Complexes and Some Related Compounds. *J. Chem. Soc.* **1959**, 3178–3182.

(56) Roe, D. M.; Massey, A. G. Perfluorophenyl Derivatives of the Elements XXVI. Tetrafluorobenzobarrelene Complexes of Mn, Co, Rh, Pd and Pt. *J. Organomet. Chem.* **1971**, *28*, 273–279.

(57) Falcon, M.; Farnetti, E.; Marsich, N. Stereoselective Living Polymerization of Phenylacetylene Promoted by Rhodium Catalysts with Bidentate Phosphines. *J. Organomet. Chem.* **2001**, *629*, 187–193.

(58) Ulmer, L.; Mattay, J.; Torres-García, H. G.; Luftmann, H. The Use of 2-[(2E)-3-(4-Tert-Butylphenyl)-2-Methylprop-2-Enylidene]-Malononitrile (DCTB) as a Matrix for Matrix-Assisted Laser Desorption/Ionization Mass Spectrometry. *Eur. J. Mass Spectrom.* **2000**, *6*, 49–52.

(59) Sedlacek, J.; Vohlidal, J.; Grubisic-Gallot, Z. Molecular-weight Determination of Poly(phenylacetylene) by Size-exclusion Chromatography/low-angle Laser Light Scattering. Influence of Polymer Degradation. *Makromol. Chem., Rapid Commun.* **1993**, *14*, 51–53.

(60) Percec, V.; Rudick, J. G. G. Independent Electrocyclization and Oxidative Chain Cleavage along the Backbone of cis-Poly(phenylacetylene). *Macromolecules* **2005**, *38*, 7241–7250.

(61) Podzimek, S. *Light Scattering, Size Exclusion Chromatography and Asymmetric Flow Field Flow Fractionation*; John Wiley and Sons: Hoboken, New Jersey, 2011; pp 65–72.

(62) SAINT+, version 6.01: Area-Detector Integration Software; Bruker AXS: Madison, WI, 2001.

(63) SADABS, *Area Detector Absorption Correction Program*; Bruker AXS: Madison, WI, 1996.

(64) Sheldrick, G. M. Phase Annealing in SHELX-90: Direct Methods for Larger Structures. *Acta Crystallogr., Sect. A: Struct. Sci., Cryst. Eng. Mater.* **1990**, *46*, 467–473.

(65) Sheldrick, G. M. A Short History of SHELX. *Acta Crystallogr., Sect. A: Struct. Sci., Cryst. Eng. Mater.* **2008**, *64*, 112–122.

(66) Sheldrick, G. M. Crystal structure refinement with SHELXL. *Acta Crystallogr., Sect. C: Struct. Sci., Cryst. Eng. Mater.* **2015**, *71*, 3–8.

(67) Farrugia, L. J. WinGX and ORTEP for Windows: an update. *J. Appl. Crystallogr.* **2012**, *45*, 849–854.